arXiv:astro-ph/0009084v1 6 Sep 2000

A grid of composite models for the simulation of the emission-line spectra from the NLR of active galaxies

.

M. Contini[1] and S.M. Viegas[2]

[1] School of Physics and Astronomy, Tel-Aviv University, Ramat-Aviv, Tel-Aviv, 69978, Israel
[2] Istituto Astronômico e Geofísico, USP, Av. Miguel Stefano, 4200,04301-904 São Paulo, Brazil

Running title : Grid of models for the NLR of Seyfert galaxies spectra

subject headings : galaxies : nuclei - galaxies : Seyfert - shock waves - model calculation

Abstract

A grid of composite models for the narrow line region of active galaxies, which consistently account for both the effect of a photoionizing radiation from the active center and of a shock front, is presented. Theoretical results, calculated with the SUMA code, are given for different values of shock velocities, preshock densities, geometrical thickness of the clouds, and, particularly, for the ionizing radiation intensity in a large range. The input parameters are chosen within the ranges indicated by previous fits of several observed emission-line and continuum spectra from active galaxies. Shock velocities from 100 $\mathrm{km\,s^{-1}}$ to 1500 $\mathrm{km\,s^{-1}}$ and preshock densities from 100 $\mathrm{cm^{-3}}$ to 1000 $\mathrm{cm^{-3}}$ are considered. The line intensities of the most important ultraviolet, optical and infrared transitions are obtained and are listed in several tables.

1 Introduction

The narrow line region (NLR) of active galactic nuclei (AGN) has a complex structure. The emission-line ratios also indicate that a variety of cloud densities and sizes are present in the NLR. The observed full width at half maximum (FWHM) of the emission-line profiles show that clouds with relatively high velocity coexist with those with lower velocities (by a factor ≥ 10). On the other hand, the radiation intensity, coming from the active center and reaching the NLR clouds, decreases with the distance from the central source. Therefore, only in very seldom cases the spectrum emitted from the NLR can be simulated by using an unique set of parameters. Generally, the emitted spectrum can be fitted by a weighted average of single-cloud spectra showing different characteristics (Contini 1997, Contini, Prieto & Viegas 1998a,b, Contini & Viegas 1999, Contini & Viegas 2000, Contini, Viegas & Prieto 2000).

Nevertheless, a grid of model calculations can be helpful to set the first basic conditions in the different observed regions. Although photoionization is the main process powering the NLR, shocks cannot be neglected in the study of the AGN spectra (e.g. Viegas-Aldrovandi & Contini 1989). Therefore, the grid of models presented in this paper should be used to complete the informations which were obtained until now from the diagrams by Osterbrock, Tran & Veilleux (1992). In the present calculations the effect of the shock is coupled to the effects of photoionization. Usually, in the observed spectra, the line characteristics coming from the shocked and from the photoionized zones may not be easily recognizable, since the two regions may interact through the diffuse radiation. Thus, the resulting line intensities are not just a sum of the line intensities produced in each zone, but correspond to values that are obtained by self-consistent calculations which account for the interaction of the two regions when computing the cloud physical conditions.

These new theoretical data enlarge the range of the results given by Viegas-Aldrovandi & Contini (1989), which presented a smaller number of emission-lines. In this paper, the input parameters are chosen within the range inferred from the fit of different galaxy spectra (e.g. Contini, Prieto, & Viegas 1998a,b, Contini & Viegas 2000, Contini, Viegas, & Prieto 2000).

A larger number of emission-lines in the UV-optical-IR spectral ranges are presented because: (1) different lines from the same multiplet reveal the temperature and density conditions of the emitting gas; (2) lines produced by different ions of a same element are important to constrain the intensity of the active center (AC) radiation, and (3) lines from a same ion but in the different wavelength ranges give further information on the physical conditions of the emitting region.

The single-cloud simulations are obtained with the SUMA code (see, for instance, Viegas & Contini 1994). Notice that the simulations apply whether the shocks originate from an interaction of the emitting clouds with a radio jet or from a radial outflow of the clouds across a lower density gas.

2 The grid

In our model, the clouds are moving outwards from the galaxy center. Therefore the shock forms on the outer edge of the cloud whereas the ionizing radiation reaches the opposite edge, which faces the active center.

A plane-parallel geometry is adopted. In order to calculate the physical conditions of the emitting gas, the cloud is divided in a large number of slabs. In each slab, the fractional abundances of the ions of each chemical element are calculated by solving the ionization equilibrium equations, coupled to the energy balance equation. The ionization rates due to all the ionizing mechanisms, as well as all recombinations rates, are included in the calculations (see, for instance Osterbrock 1989). In particular, the ionization due to the primary radiation (from the central source), to the diffuse radiation, generated by the free-free and free-bound transitions of the shocked and photoionizad gas, as well as the collisional ionization, are all accounted for. Because the shock front and the ionizing radiation act on the opposite edges of the cloud, the calculations imply some iterations. The gas entering the shock front is thermalized to high temperature, which depends on the shock velocity. Then, throughout the cloud, in each slab the temperature is calculated either by the enthalpy equation in the region close to the shock or by thermal equilibrium further on, where radiation processes prevail. The cooling and heating rates, which depend strongly on the gas density, determine the temperature in each slab. The geometrical thickness of the slabs is automatically calculated in order to obtain a smooth gradient of the temperature throughout the cloud. The density within each slab is calculated by the compression equation. Thus, in order to define the density distribution across the cloud, the first run starts at the shocked edge. The next iteration starts at the inner edge of the cloud reached by the ionizing radiation from the active center, ends at the shocked zone, and the physical conditions of the gas are calculated across the cloud. As in the first iteration, the third iteration starts at the shock front. After recalculating the physical condition across the cloud, the emission-line and continuum spectra are computed. Since the density is low, we assume that gas is optically thin to the emission-lines.

Depending on the geometrical thickness of the cloud, the diffuse radiation may bridge the radiation-dominated and the shock-dominanted sides. Thus, usually the cloud models are matter-bounded, unless the geometrical thickness is very large, allowing for a neutral hydrogen column density larger than 10^{18} cm^{-2} both in the shocked and photoionized zones.

The input parameters for a single-cloud model are the shock velocity, $\mathrm{V_s}$, the preshock density, $\mathrm{n_0}$, the preshock magnetic field, $\mathrm{B_0}$, the ionizing radiation spectrum, the chemical abundances, the dust-to-gas ratio by number, d/g, and the geometrical thickness of the clouds, D. A power-law, characterized by the power index α and the flux, $\mathrm{F_h}$, at the Lyman limit, reaching the cloud (in units of cm^{-2} s^{-1} eV^{-1}) is generally adopted. For all the models, $\mathrm{B_0} = 10^{-4}$ gauss, $\alpha_{UV} = 1.5$, and $\alpha_X = 0.4$, and cosmic abundances (Allen 1973) are adopted. Actually, the basic models are calculated with $\mathrm{d/g} = 10^{-15}$.

The emission-line intensities, relative to Hβ, are presented in Tables 1 to 12. Each table corresponds to a different set of input parameters $\mathrm{V_s}$, $\mathrm{n_0}$, and D. The results correspond to models with increasing ionizing flux, from the shock-dominated case (SD), which is calculated assuming $\mathrm{F_h}$=0, up to highly radiation-dominated models (RD) for which log $\mathrm{F_h}$ can reach up to 12.48. The UV and optical emission-lines, relative to Hβ, are listed in the top part of the tables, while the near-infrared (NIR) and IR emission-line ratios appear in the bottom. The absolute Hβ value is also listed.

Two cases of cloud geometrical thickness are presented: (a) D=10^{17} cm, which corresponds to matter-bounded models, and (b) D=10^{19} cm, corresponding to radiation-bounded models. Notice, however, that for models with $\mathrm{V_s}$=500 $\mathrm{km\,s^{-1}}$ and $\mathrm{n_0}$=300 cm^{-3}, the results for matter-bounded models are obtained with 10^{18} cm, because for D=10^{17} cm the cloud is fully ionized with $\mathrm{T} > 3.\ 10^6$ K, reducing the intensity of most of the emission-lines to zero.

Also for models with $\mathrm{V_s}$=200 $\mathrm{km\,s^{-1}}$and $\mathrm{n_0}$=200 cm^{-3}, the lowest D is 10^{18} cm, in order to find out the critical D in the low velocity-density models. In fact, Tables 1 to 4 refer to low preshock densities and velocities (n_0 = 100 - 200 cm^{-3}, V_s= 100 - 200 $km\,s^{-1}$). Tables 5 to 10 show the results obtained for different V_s and a constant n_0 = 300 cm^{-3}. Notice that, besides the adiabatic jump at the shockfront, the gas is compressed downstream depending on V_s, reaching the densities which are generally observed in the NLR of AGN.

The results for high velocity shock-dominated clouds appear in Tables 11 and 12. For these models, the line ratios are given for different distances from the shock front, in the region where the gas temperature is rapidly decreasing, as shown by the temperature of the corresponding slab, which is also listed in the tables. Notice, however, that the line intensities listed correspond to the result of the integration across the cloud, and not only to the slab contribution. Except for model 88 (Table 11), which represents the case of a high V_s (1500 $km\,s^{-1}$) and low n_0 (300 cm^{-3}), all the other models correspond to high V_s and high n_0, since we are assuming that V_s and n_0 dependence with the distance from the center follows the observed general trend from the BLR (high velocity and density clouds closer to the center) to the NLR (lower velocity and density farther from the center).

In Table 13 the maximum value of the downstream densities and temperatures are given for each model, which is identified by the shock velocity (first column) and by the preshock density (second column).

In Table 14 some significative line ratios for SD models are presented. When the values for small ($10^{17} - 10^{18}$ cm) and large (10^{19} cm) D are very similar only one value is given. In the opposite case, the first value refers to small D and the second to large D.

3 Comments

The results from SD and RD models are very different. Particularly, the Hβ absolute value is very low in SD models compared to RD models. Recall that photoionization is generally an efficient mechanism for ionizing the gas, while shocks are more efficient heating the gas. Thus, the shocked zone is usually at a higher temperature and has a H^+ emitting zone smaller than the photoionized region. Both conditions do not favor recombination lines, so, the H lines are less intense, and the luminosity of Hβ coming from the shocked gas is lower.

The RD models are composite, because they contain also the contribution of the shocked gas. The calculated absolute line intensity corresponds to the value at the NLR. Any average spectrum must be obtained from weighted single-cloud models. The weights correspond to the single-cloud areas. In order to compare to the observed (at Earth) absolute flux, the dilution due to the distance must be taken into account.

3.1 SD models

UV lines

For V_s= 200 - 300 $km\,s^{-1}$, OVI/Hβ is maximum . The temperatures downstream are 6 10^5 - 1.4 10^6 K, whereas the postshock densities ($\geq 10^3 - 10^4$ cm^{-3}) are low enough and the cloud has a large high temperature zone. For the emission-lines NV, SiIV, OIV, NIV] and CIV, and SiIII, relative to Hβ, the maximum value occurs for V_s=200 $km\,s^{-1}$. However, in the matter-bounded case (D=10^{17} cm), the line ratios are also high for V_s=100 $km\,s^{-1}$, since models where a large zone of emitting gas at T$\geq$ 10^4 K is cut out from the cloud favor the high ionization lines as compared to Hβ.

The models with those velocities are radiation-bounded for D slightly larger than D=10^{18} cm. In fact, the results shown in Tables 3 and 4 are very similar. The values of Lyα/Hβ are very sensitive to D and have a maximum at V_s=200 $km\,s^{-1}$. On the other hand, HeII 1640/Hβ is rather low in SD models and reaches a maximum value of 2.7 for V_s=300 $km\,s^{-1}$.

Optical lines

The lowest value of the [OIII] 5007+4959/[OII] 3727 line ratio is shown by SD models (see Table 14), whereas the lines from the first ionized ions ([NII], [SII], FeII, SiII, [SiII], etc.) are generally strong. The [OIII]/[OII] line ratio becomes larger than unit for $V_s\geq$ 300 $km\,s^{-1}$.

Values of [OIII]5007+4959/[OIII]4363 line ratio are very low ($<$ 20), which are characteristic of LINERs (see, e.g., Contini 1997). This line ratio decreases with increasing temperature and density of the emitting gas. Table 14 shows an opposite trend, i.e. an increasing line ratio with increasing V_s and n_0. This is due to the fact that, at higher V_s, higher ionization states of O, collisionally ionized, dominate the postshock zone, which is at higher temperature, whereas the O^{+2} ion is mainly present in the gas at lower temperature, where ionization by the diffuse radiation dominates.

Neutral lines such as [OI] and [NI] lines, are relatively strong. On the other hand, high-ionization lines, relative to Hβ, as [FeVII, [FeX] and [FeXI] peak at V_s=300 $km\,s^{-1}$, $V_s>$ 500 $km\,s^{-1}$, and V_s = 1500 $km\,s^{-1}$, respectively.

Another important issue, particularly raised in the case of NGC 4151 (Contini, Viegas, & Prieto, 2000), refers to the [OIII]5007+4959/[OII]3727 line ratio. It is argued whether this ratio increases faster with n_0 (for a fixed V_s= 200 $km\,s^{-1}$) or with V_s (for a fixed n_0 = 200 cm^{-3}). In the latter case the density increases downstream because compression increases with V_s. It can be seen in Fig. 1 that the slope is flatter for models calculated as function of the preshock density n_0. This indicates that, in the range of the corresponding downstream densities, compression due to V_s prevails over the effect of a higher n_0 . As shown in Table 13, a model with a higher n_0 (300 cm^{-3}) and a lower V_s (100 $km\,s^{-1}$) leads to a lower density downstream than a model with a higher n_0 (200 cm^{-3}) and lower V_s (200 $km\,s^{-1}$). Therefore, lower [OIII]/[OII] corresponds to a lower n_0 and/or to a lower V_s.

IR lines

Most of the coronal lines are in the NIR range. They become observable for $V_s \geq 200$ $km\,s^{-1}$ and their intensities increase with V_s reaching a maximum at 1500 $km\,s^{-1}$. On the other hand, lower ionization lines are strong at low V_s. Notice that high values for [FeII]26/Hβ, [SiII]34.8/Hβ, [NeII]12.8/Hβ, and [OI]63/Hβ are obtained with V_s=100 $km\,s^{-1}$, n_0=100 cm^{-3}, and D=10^{19} cm (Table 2). These input parameters favor the formation of a large low-ionization zone in a shocked cloud. We have chosen the infrared [SiIX]/[SiVII] and [NeIII]/[NeII] line ratios as indicative of SD models (see Table 14).

High velocity models

High velocity shocks correspond to high temperatures in the postshock region. For 1000 $km\,s^{-1}$ and 1500 $km\,s^{-1}$, the temperature reaches 1.5 10^7 K and 3.5 10^7 K, respectively. If present in the NLR, such high velocity clouds may contribute to the observed X-ray emission-lines and soft X-ray continuum. By cutting the cloud at different distances from the shock front, different matter-bounded models can be obtained and very different spectra can be generated, because the fractional abundances of the ions of a given element peak at different temperatures.

However, the strong compression, due to high V_s, coupled to high n_0, leads to a high cooling rate and a drastic change in the temperature. The jump of the physical conditions can reduce the volume of gas with temperatures between 10^4 and 10^6 K (Tables 11-12). Thus, most of the intermediateionization lines can be drastically reduced. Recall that the intensity of a line depends on the volume of gas with the ideal physical conditions to emit it.

3.2 RD composite models

Lines from different ionization stages peak for different values of F_h. However, in some cases, the line intensity ratios have no simple dependence on F_h because the effect of the shock, modifying the stratification of the ions downstream (see, e.g., Contini & Viegas 1991), interacts with the effect of the primary and diffuse ionizing radiation.

High ionization lines (e.g., OVI and NV in the UV, coronal lines in the NIR, etc.) can be strong only for very high F_h and $V_s \geq 200$ km s^{-1} (e.g., Table 4, model 39, and Table 9, model 76).

In the optical range, [FeVII]/Hβ peaks at the highest value of F_h except for the models with V_s=100 km s^{-1} where the maximum is reached for $\log(F_h) = 10.48$ and 11.48 whether D is equal to 10^{17} cm or to 10^{19} cm, respectively. Notice that [FeX] and [FeXI] follow a similar trend. As expected, the infrared low ionization [FeII] 26 line decreases with F_h for all V_s.

The most significant optical line ratios are given as function of log F_h for different values of V_s in Figs. 2, 3, and 4. The [OIII]/[OII] ratio is basically used for modeling, as an ionization indicator, because both lines are generally observed and strong. Notice the increasing trend of this line ratio with increasing F_h, for all models with $V_s < 300$ km s^{-1}. The same trend appears for models with $V_s \geq 300$ km s^{-1}and high D. Comparing to the results plotted in Fig. 1, which refers to SD models, we see that the [OIII]/[OII] line ratio is much more sensitive to the intensity of the flux radiation from the AC than to the shock velocities.

The [SII] line ratio reveals the density of the emitting gas. Because of the low critical density of the [S II] lines, only models with n_0=100 and 200 cm^{-3} can have [SII]6717/6730 ≥ 1 (Fig. 3).

The [OIII]5007+4959/[OIII]4363 line ratio is a temperature indicator and is used to distinguish between shock dominated and radiation dominated models (Fig. 4).

When the effect of photoionization and shock are both taken into account, some results may not be so obvious. For example, the behaviour of the [O III] line ratio, which can be higher for higher n_0 and V_s, as shown in Fig. 4, or the behavior of the [Fe VII] 6087 with D.

For sake of clarity and understanding, the distributions of the electron density and temperature across the cloud are shown in Figs. 5a, 6a, and 7a for three different models (top panel), as well as the ion fractional abundances of H^{+1}, O^{+2}, Fe^{+6}, Fe^{+9}, and Fe^{+10} (bottom panel). Some ionization rates are plotted in Figs. 5b, 6b, and 7b.

The shockfront is on the right and the cloud edge reached by the photoionizing flux on the left.

Figs. 5a and b refer to model 69 (V_s=300 km s^{-1}, n_0=300 cm^{-3}, D=10^{19} cm, and log F_h=12). These figures can help to understand the rather high [OIII] 5007+4959/4363 line ratios found in some models. It can be seen that the [OIII] lines are emitted from a region where a lukewarm gas is mainly ionized by primary and diffuse radiation, while higher ionization ions, like Fe^{+6}, Fe^{+9}, and Fe^{+10}, appear at the high temperature postshock zone.

Fig. 5c refers to the SD model 63 (V_s=300 km s^{-1}, n_0=300 cm^{-3}). The [OIII] lines are emitted in the region where the high postshock temperature is rapidly dropping to lower values. In this case 5007/4363 ratio is very low ($\sim$ 12) reflecting the shock effect on the gas temperature. Comparison to Fig. 5a, where the bulk of O^{+2} is at lower temperature, can explain the behavior of the 5007/4363 ratio in RD and SD models.

Figs. 6 and 7 correspond to models 28 (D=10^{18} cm) and 37 (D=10^{19} cm), respectively, both with V_s=200 km s^{-1}, n_0=200 cm^{-3}, and log F_h=11.78, illustrating the differences for narrow and wide cloud models. Notice that for both models an extended zone of lurkewarm gas (T of the order of 10^4 K) appears in the internal region of the cloud. However, on closer inspection, comparing the temperature and O^{+2} distributions in Figs 6 and 7, we see that the [OIII] lines are emitted from a gas at a lower tamperature in a wide cloud than in a narrower cloud. Therefore, the [OIII] 5007/4636 line ratio is lower for small D models.

When the shock velocity is high enough, the high ionization lines come from both sides of the cloud, i.e., from the hot postshock zone and from the slabs closer to the photoionized edge. Because the high ionization zones are closer to the edges, their volumes are less affected than the volume of the low ionization zone by a decrease of the cloud geometrical thickness. We can say that the emitting volume of the low ionization lines decreases faster with the geometrical thickness of the cloud than that of the high ionization lines. On the other hand, Hβ is produced across the whole cloud, thus the high-ionization line intensity, relative to Hβ increases while the Hβ absolute flux decreases. As an example, we can compare the results of [Fe VII] 6087 given by models 28 and 37, which differ only by the value of D, respectively, 10^{18} cm and 10^{19} cm. The [Fe VII]/Hβ ratio decreases from model 28 to 37, while Hβ absolute flux increases. The net effect is a decrease of the absolute flux of [Fe VII] from model 28 to 37.

Figs. 6b and 7b show that in the immediate postshock region collisional ionization prevails because of its exponential dependency on the temperature. After the rapid decrease of the temperature downstream, the primary ionization rate dominates throughout the cloud. The fractional abundance of Fe^{+6} is never negligible throughout the whole cloud for small D (Fig. 6a), whereas it can be low in the internal zone of a wide cloud (model 37, D=10^{19} cm), depending on the primary radiation rate. The temperatures reached in the radiation dominated side (left) of the cloud are lower in the wide cloud model ($\leq$ 1.82 10^4 K) than in the narrower one ($\leq$ 2.23 10^4 K). Both values are in a range which is crucial with respect to rapid variations in the interplay between ionization and recombination coefficients.

4 Suggestions

Let us conclude by describing the method we have used in the last few years in order to successfully modeling the NLR spectra of Seyfert galaxies.

First, we chose the V_s corresponding to the FWHM of the observed line profiles. On this basis, we chose the model fitting the most important lines, which are usually those with the lowest observed uncertainty. Then, we add other models with different weights to improve the fitting of all the other observed emission-lines. Following this procedure, we obtain a picture of the physical conditions in the NLR of the galaxy. Notice, however, that each galaxy is a special case. So, this grid must be used only as a first approach to explain the observed spectrum.

In order to have a full description of the NLR, the models fitting the emission-line spectrum must also explain the observed continuum spectrum. This may force the inclusion of new components (clouds under different physical conditions), which must be tested against the observed emission-line spectrum. The process may be repeated until both the emission-line and continuum spectra are fitted. Once the fit is achieved, all the information about the clouds present in the NLR is available, including the relative importance of their contribution to the emission in each spectral range.

Acknowledgements: We are grateful to the referee for enlightening comments. This paper is partially supported by CNPq (304077/77-1), PRONEX/Finep (41.96.0908.00), and FAPESP (97/13861-4).

References

Allen, C.W. 1973, Astrophysical Quantities (London: Athlone)
Contini, M. 1997, A&A, 323, 71
Contini, M. & Viegas, S.M. 1991, A&A 251, 27
Contini, M. & Viegas, S.M. 1999 ApJ, 523,114
Contini, M. & Viegas, S.M. 2000 ApJ, 535,
Contini, M., Prieto, M.A., & Viegas 1998a ApJ , 492, 511
Contini, M., Prieto, M.A., & Viegas 1998b ApJ , 505, 621
Contini, M. Viegas, S.M., & Prieto, M.A. 2000 ApJ submitted
Nelson, C.H. et al astro-ph/9910019
Osterbrock, D. E. 1989, "Astrophysics of Gaseous Nebulae and Active Galactic Nuclei" (University Science Books)
Osterbrock, D.E., Tran, K.D., & Veilleux, S. 1992, ApJ, 389, 1960
Viegas-Aldrovandi, S.M. & Contini, M. 1989, ApJ 339, 689
Viegas, S.M. & Contini, M. 1994, ApJ, 428, 113

Figure Caption

Fig. 1 :

Emission line ratios as a function of V_s (dashed lines, labelled by n_0) and n_0 (solid lines, labelled by V_s). Thin lines correspond to [OIII]5007+4959/[OII]3727 and thick lines to [OII]3727/Hβ.

Fig. 2 :

The [OIII]5007+4959/[OII]3727 emission-line ratio versus log F_h, for models with: V_s=100 $km\,s^{-1}$and n_0=100 cm^{-3} (solid lines), V_s=100 $km\,s^{-1}$and n_0=300 cm^{-3} (dot-dashed lines), V_s=200 $km\,s^{-1}$(dotted lines), V_s=300 $km\,s^{-1}$(short-dashed lines), and V_s=500 $km\,s^{-1}$(long-dashed lines). Thin lines refer to results for D=10^{17}-10^{18} cm, whereas thick lines, to D=10^{19} cm.

Fig. 3 :

The [SII]6717/[SII]6730 emission-line ratio versus log F_h. Same notation as in Fig. 2.

Fig. 4 :

The [OIII]5007+4959/[OIII]4363 emission-line ratio versus log F_h. Same notation as in Fig. 2.

Fig. 5

Results from Model 69 (V_s= 300 $km\,s^{-1}$, n_0=300 cm^{-3}, D=10^{19} cm, log F_h=12). The shocked edge is on the right and the ionized edge on the left. (a) : the distribution across the cloud of the temperature (dashed line) and density (solid line) in the top panel, and of the fractional abundances of the H^{+1} (solid), O^{+2} (dot-dashed), Fe^{+6} (dotted), Fe^{+9} (short dashed), and Fe^{+10} (long-dashed) ions (bottom panel).

(b) : the distribution across the cloud of the collisional (dotted), diffuse from the shockfront (long-dashed), diffuse from the edge reached by the photoionizing radiation from the center (dash-dotted), and primary (short-dashed) ionization rates for the O^{+2} ion.

(c) : same as for (a) in the shock dominated case.

Fig. 6

Results from Model 28 (V_s=200 $km\,s^{-1}$, n_0=200 cm^{-3}, D=10^{18} cm, log F_h=11.78). (a) Same notation as in Figs. 5a; (b) same notation as in Fig. 5b, but for Fe^{+6} ionization rates.

Fig. 7

Results from Model 37(V_s= 200 $km\,s^{-1}$, n_0=200 cm^{-3}, D=10^{19} cm, log F_h=11.78). Same notation as in Figs. 6.

Fig.1

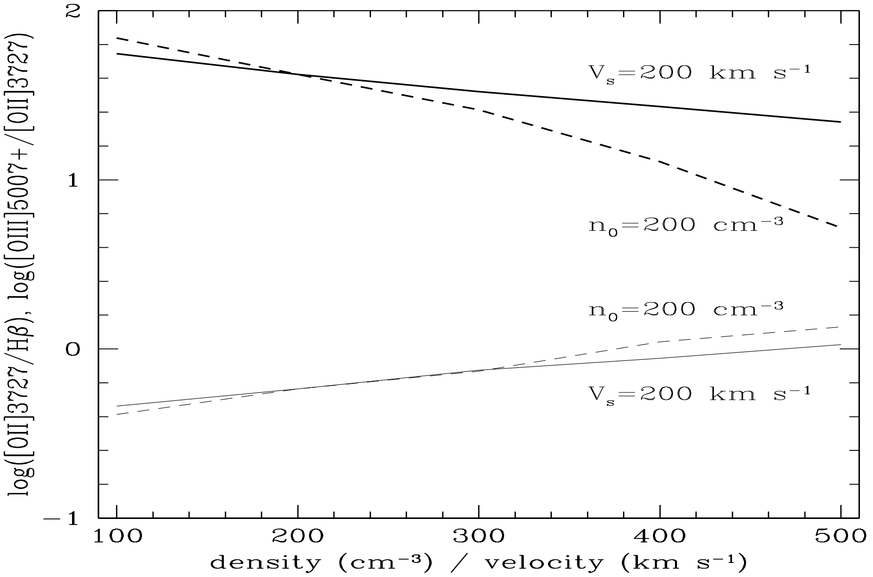
log([OII]3727/Hβ), log([OIII]5007+/[OII]3727)
2
1
0
−1
100
200
300
400
500
density (cm⁻³) / velocity (km s⁻¹)
Vs=200 km s⁻¹
n0=200 cm⁻³
n0=200 cm⁻³
Vs=200 km s⁻¹

Fig.2

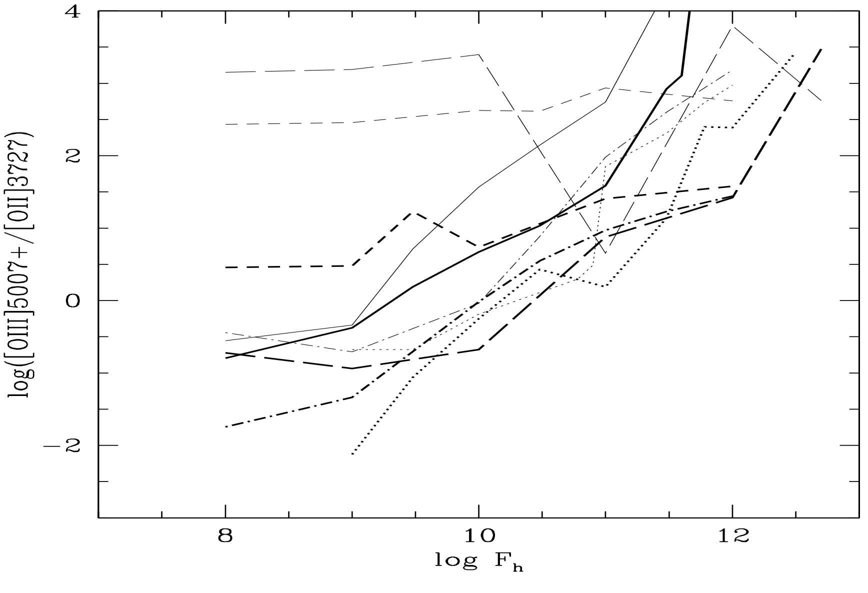
log([OIII]5007+/[OII]3727)
4
2
0
−2
8
10
12
log Fh

Fig.3

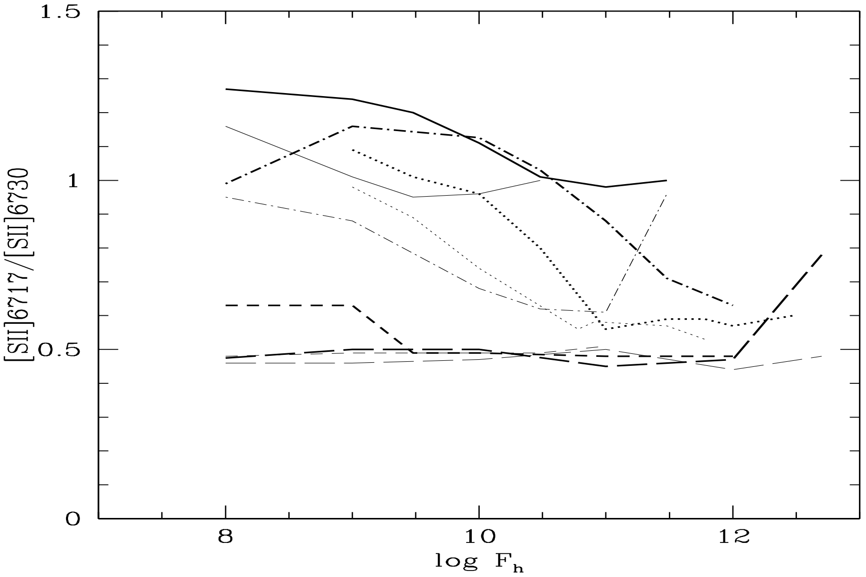

1.5
1
0.5
0
[SII]6717/[SII]6730
8
10
12
log F_h

Fig.4

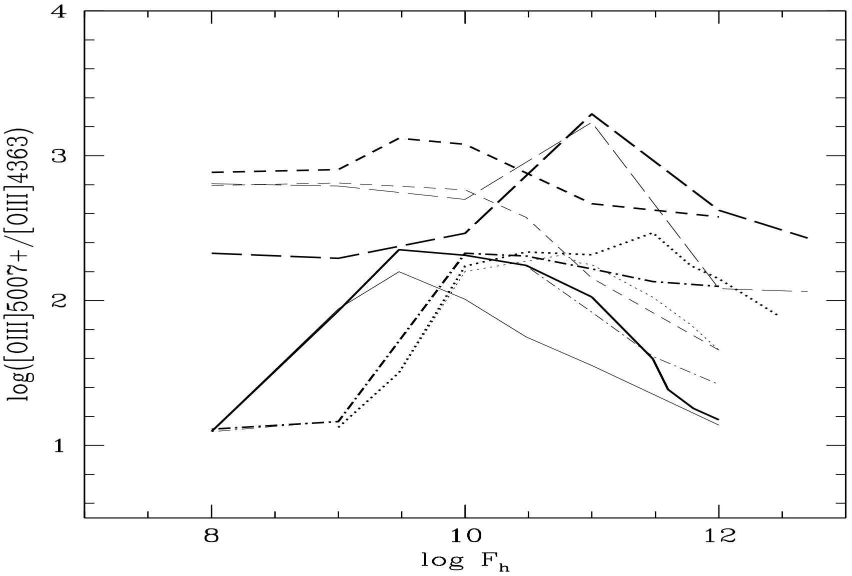

4
3
2
1
log([OIII]5007+/[OIII]4363)
8
10
12
log F_h

Fig.5a

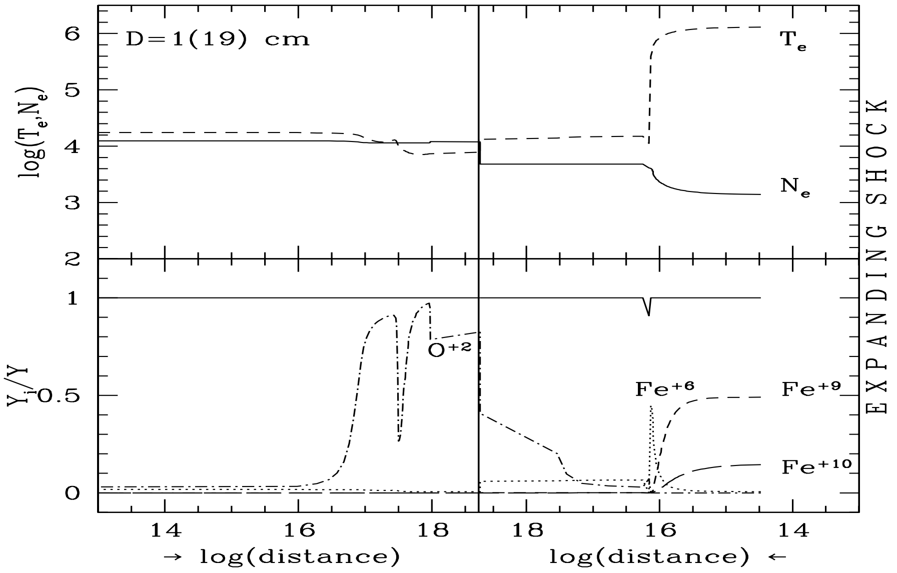

Fig.5b

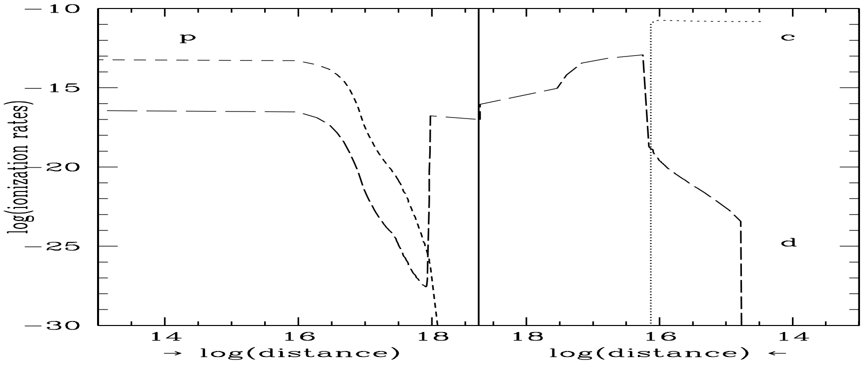

Fig.5c

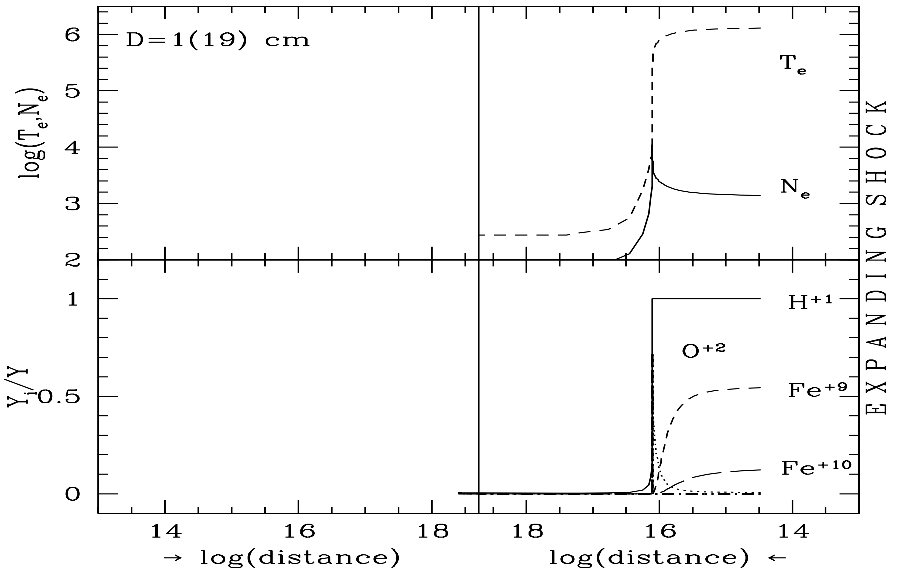

Fig.6a

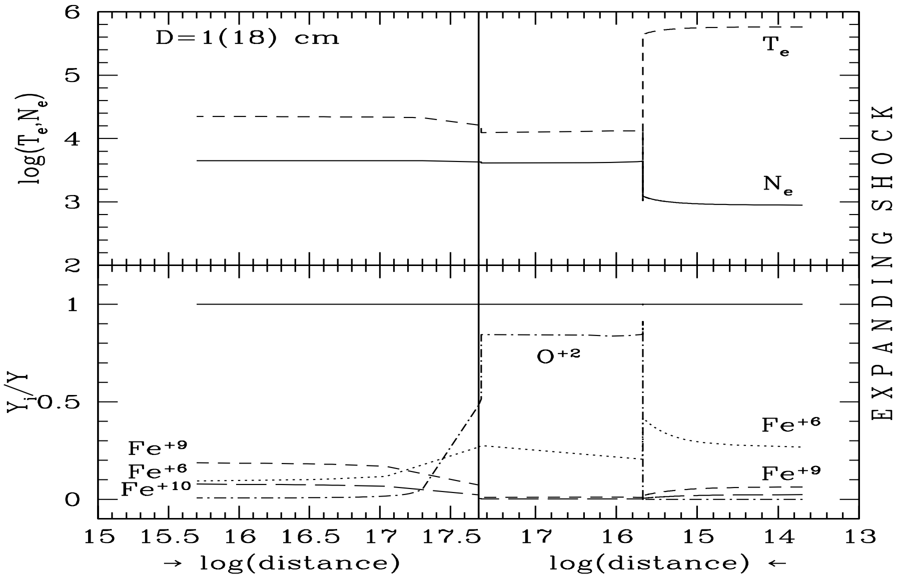

D=1(18) cm
T_e
N_e
log(T_e,N_e)
EXPANDING SHOCK
Y_i/Y
O^{+2}
Fe^{+9}
Fe^{+6}
Fe^{+10}
Fe^{+6}
Fe^{+9}
6
5
4
3
2
1
0.5
0
15
15.5
16
16.5
17
17.5
17
16
15
14
13
→ log(distance)
log(distance) ←

Fig.6b

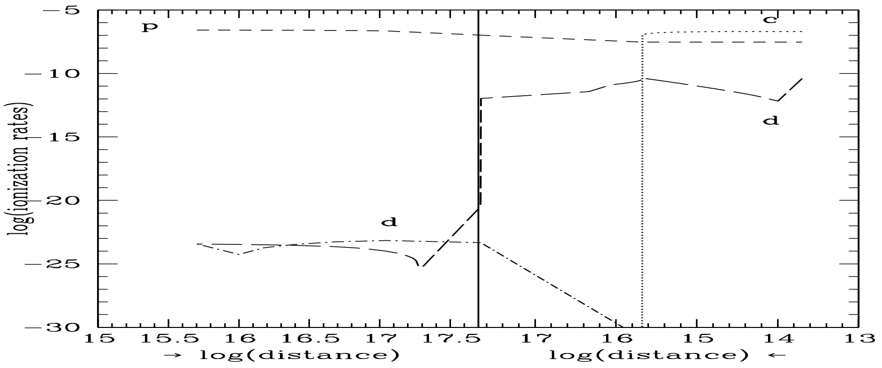

p
c
d
d
log(ionization rates)
−5
−10
15
−20
−25
−30
15
15.5
16
16.5
17
17.5
17
16
15
14
13
→ log(distance)
log(distance) ←

Fig.7a

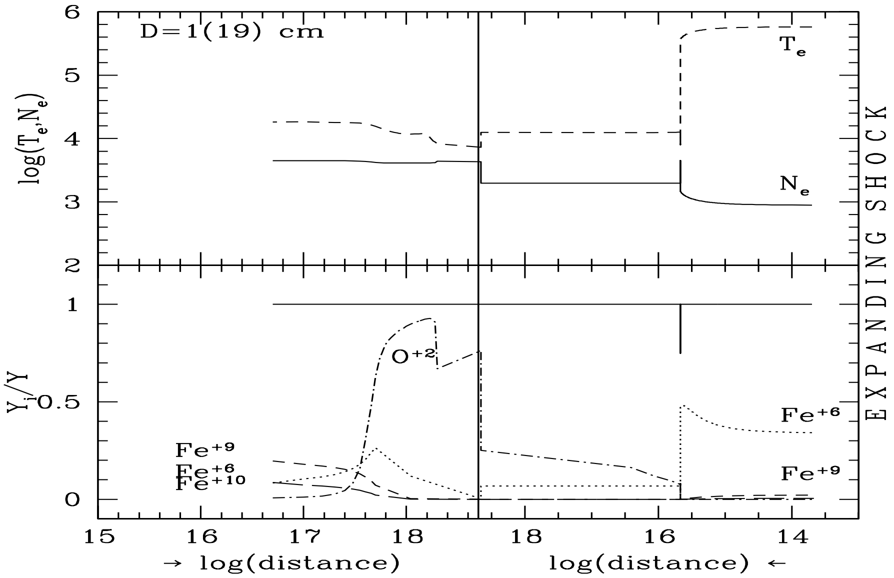

D=1(19) cm
T_e
N_e
$\log(T_e,N_e)$
EXPANDING SHOCK
Y_i/Y
O^{+2}
Fe^{+9}
Fe^{+6}
Fe^{+10}
Fe^{+6}
Fe^{+9}
6
5
4
3
2
1
0.5
0
15
16
17
18
18
16
14
→ log(distance)
log(distance) ←

Fig.7b

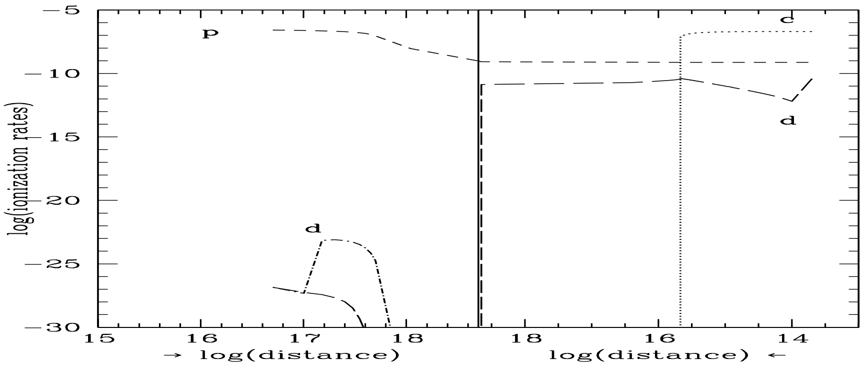

p
c
d
d
log(ionization rates)
−5
−10
15
−20
−25
−30
15
16
17
18
18
16
14
→ log(distance)
log(distance) ←

Table 1

The models : V_s=100 $\mathrm{km\,s^{-1}}$, n_0=100 $\mathrm{cm^{-3}}$, D= 10^{17}cm

		1	2	3	4	5	6	7	8
log F_h		SD	8	9	9.48	10	10.48	11	12
O VI	1033	0.024	0.007	0.005	0.0096	0.08	1.38	20.2	178.8
Si III	1206	21.9	2.97	0.26	0.07	0.033	0.017	0.0016	0.0
H I	1216	133.	38.	27.3	24.	23.9	24.4	25.7	31.5
N V	1240	3.97	0.56	0.07	0.053	0.15	1.17	7.27	6.8
S II	1256	2.0	0.28	0.033	0.008	0.0035	5.8(-4)	0.0	0.0
Si II	1264	0.5	0.07	0.008	0.0029	8(-4)	2.1(-4)	1.5(-5)	0.0
O I	1302+	0.049	0.0072	0.0019	1.(-4)	2.6(-5)	3.3(-6)	0.0	0.0
Si IV	1397	13.6	1.83	0.15	0.055	0.138	0.156	0.02	0.0
O IV	1401+	29.	4.1	0.48	0.37	0.78	3.54	5.5	0.6
N IV]	1486	17.	2.5	0.29	0.19	0.45	2.1	4.	0.3
C IV	1550	102.	14.2	1.65	1.09	3.35	14.5	22.9	2.8
He II	1640	0.27	0.5	1.2	2.13	5.7	7.4	8.0	9.14
Si III	1892+	18.6	2.53	0.27	0.37	0.45	0.12	0.004	0.0
[Ne V]	3426	0.037	0.005	0.0013	0.007	0.31	3.0	7.6	1.12
[O II]	3727	68.	13.1	8.3	3.6	0.72	0.08	0.0026	0.0
[Ne III]	3869+	2.76	0.77	0.86	1.16	1.4	0.52	0.053	0.0
[S II]	4073+	0.63	0.33	0.22	0.0085	0.0017	0.0	0.0	0.0
[O III]	4363	2.08	0.29	0.044	0.117	0.26	0.2	0.04	2.9(-4)
He II	4686	0.024	0.077	0.18	0.32	0.83	1.04	1.03	0.9
[O III]	5007+	25.9	3.67	3.86	18.5	26.6	11.2	1.43	0.004
[N I]	5200+	0.17	0.035	0.0033	3.5(-4)	2.5(-5)	0.0	0.0	0.0
He I	5876	0.81	0.25	0.14	0.1	0.036	0.008	0.0018	2(-4)
[Fe VII]	6087	0.0038	7.1(-4)	4.4(-4)	0.0034	0.24	0.91	0.4	0.002
[O I]	6300+	0.41	2.17	0.84	0.009	1.8(-4)	0.0	0.0	0.0
[Fe X]	6374	0.0	0.0	0.0	2.(-7)	2.6(-4)	0.018	0.35	0.2
[N II]	6548+	7.64	7.81	5.	1.44	0.24	0.03	0.001	0.0
[S II]	6716	2.4	3.73	2.21	0.21	0.0082	1.3(-4)	0.0	0.0
[S II]	6731	2.3	3.2	2.19	0.22	0.0085	1.25(-4)	0.0	0.0
[O II]	7325	5.3	0.79	0.25	0.11	0.03	0.0045	1.9(-4)	0.0
[Fe XI]	7892	0.0	0.0	0.0	0.0	1.8(-5)	0.0025	0.12	0.27
Hβ	$\mathrm{erg\,cm^{-2}s^{-1}}$	4.85(-5)	3.48(-4)	0.003	0.0052	0.0045	0.0034	0.0025	7.6(-4)
[S III]	9532+	2.42	1.28	1.17	3.4	0.66	0.018	3.6(-4)	0.0
[C I]	9850	0.56	4.(-4)	1.9(-4)	7.7(-5)	2.7(-6)	1.7(-7)	0.0	0.0
[S VIII]	9913	0.0	1.1(-6)	6.1(-6)	3.2(-5)	0.0026	0.056	0.33	0.016
[S IX]	1.25	0.0	0.0	5.7(-8)	4.6(-7)	5.2(-5)	0.0025	0.05	0.04
[Si VI]	1.96	6(-5)	4.7(-4)	5.6(-4)	0.0045	0.15	0.46	0.22	1(-4)
[Si VII]	2.48	0.0	2.8(-6)	2.3(-5)	2.2(-4)	0.02	0.23	0.47	0.0047
[Si IX]	2.59	0.0	0.0	3.5(-8)	8.2(-7)	2.6(-4)	0.024	0.78	2.02
[Mg VIII]	3.03	0.0	0.0	1.24(-8)	7.4(-7)	9.(-4)	0.048	0.59	0.61
[Si IX]	3.9	0.0	0.0	6.8(-8)	1.6(-6)	6.3(-4)	0.057	1.73	4.
[Mg VII]	5.5	0.0	1.6(-8)	9.5(-7)	3.5(-5)	0.02	0.41	1.29	0.09
[Mg V]	5.6	0.0011	2.1(-4)	2.8(-4)	0.06	0.43	0.54	0.085	2.6(-5)
[Ne VI]	7.6	6.9(-6)	3.1(-6)	1.29(-5)	6.2(-4)	0.053	0.86	4.4	2.94
[Ar III]	8.99	0.09	0.066	0.122	0.37	0.08	0.001	2(-6)	0.0
[S IV]	10.54	0.35	0.0495	0.04	1.03	2.45	0.29	0.014	0.0
[Ne II]	12.8	0.55	9.6(-6)	0.14	0.039	0.005	2.5(-4)	3.(-6)	0.0
[Ne V]	14.32	0.003	4.8(-4)	0.0017	0.051	1.47	5.94	6.08	0.17
[Ne III]	15.55	0.25	1.73	1.73	1.59	1.0	0.19	0.01	0.0
[S III]	18.7	0.222	0.53	0.36	0.96	0.14	0.0027	4.4(-5)	0.0
[Ne V]	24.3	0.004	6.3(-4)	0.0017	0.049	1.45	6.07	6.48	0.21
[O IV]	25.9	1.17	0.16	0.11	1.47	13.3	20.4	7.37	0.055
[Fe II]	26.	3.58	2.0	0.7	0.026	1.(-5)	0.0	0.0	0.0
[S III]	33.5	0.3	0.87	0.43	1.0	0.15	0.003	5(-5)	0.0
[Si II]	34.86	18.3	7.4	1.94	0.47	0.022	7.8(-4)	7.6(-6)	0.0
[Ne III]	36.01	0.02	0.15	0.15	0.139	0.088	0.017	9(-4)	0.0
[O III]	51.81	0.4	0.08	0.99	3.15	2.67	0.65	0.05	6.7(-5)
[O I]	63.18	3.27	3.36	0.38	0.0029	3.3(-5)	3.7(-8)	0.0	0.0
[O III]	88.36	0.37	0.066	0.48	1.558	1.35	0.35	0.029	4.8(-5)
[O I]	145.5	0.22	0.29	0.03	1.9(-4)	2.(-6)	2.(-9)	0.0	0.0
[C II]	157.7	1.48	0.96	0.085	0.015	0.003	2.5(-4)	1.25(-5)	0.0

Table 2

The models : V_s=100 km s^{-1}, n_0=100 cm^{-3}, D= 10^{19}cm

		9	10	11	12	13	14	15	16	17	18	19
log F_h		SD	8	9	9.48	10	10.48	11	11.48	11.6	11.8	12
O VI	1033	0.0014	3.3(-4)	6(-4)	7.1(-4)	8(-4)	0.003	0.39	45.	98.	146.5	191.
Si III	1206	1.3	0.25	0.16	0.084	0.037	0.046	0.5	0.11	6(-4)	0.0	0.0
H I	1216	37.	25.7	26.2	27.3	30.4	31.2	26.9	25.2	26.4	27.3	30.3
N V	1240	0.24	0.045	0.03	0.016	0.006	0.012	0.33	8.9	13.8	10.86	8.
S II	1256	0.12	0.023	0.017	0.013	0.016	0.03	0.16	4(-5)	0.0	0.0	0.0
Si II	1264	0.03	0.006	0.005	0.004	0.0045	0.005	0.015	9.4(-4)	0.0	0.0	0.0
O I	1302+	0.0029	9(-4)	0.0012	0.0018	0.003	0.0035	0.0013	0.0	0.0	0.0	0.0
Si IV	1397	0.8	0.15	0.1	0.05	0.018	0.008	0.076	1.1	0.008	0.0	0.0
O IV	1401+	1.8	0.32	0.2	0.12	0.05	0.065	0.55	7.	7.7	1.6	0.7
N IV]	1486	1.3	0.2	0.13	0.07	0.04	0.08	0.6	7.	5.6	1.1	0.4
C IV	1550	6.1	1.15	0.77	0.4	0.3	0.89	5.67	43.	35.5	10.7	3.9
He II	1640	0.017	0.13	0.57	1.0	1.34	1.36	1.67	5.4	8.	8.5	9.
Si III	1892+	1.11	0.21	0.15	0.16	0.4	0.88	3.67	0.2	8(-4)	0.0	0.0
[Ne V]	3426	0.0022	4.2(-4)	3.2(-4)	0.0013	0.026	0.16	0.9	5.6	6.72	3.5	1.28
[O II]	3727	4.2	1.9	4.	4.8	3.4	1.94	0.8	0.04	0.004	0.0	0.0
[Ne III]	3869+	0.167	0.167	0.5	0.94	1.45	1.49	1.85	1.94	0.1	6.4(-4)	3(-5)
[S II]	4073+	0.037	0.1	0.25	0.43	0.6	0.56	0.5	8(-6)	0.0	0.0	0.0
[O III]	4363	0.12	0.024	0.02	0.033	0.078	0.12	0.29	0.84	0.21	2(-3)	4(-4)
He II	4686	0.0015	0.02	0.089	0.16	0.2	0.2	0.23	0.66	0.95	0.96	0.9
[O III]	5007+	1.55	0.3	1.7	7.4	16.	21.	30.8	33.3	5.1	0.036	0.006
[N I]	5200+	0.01	0.25	0.18	0.17	0.06	0.0086	6.6(-4)	0.0	0.0	0.0	0.0
He I	5876	4.5	0.63	0.4	0.24	0.15	0.12	0.1	0.043	0.005	4(-4)	2(-4)
[Fe VII]	6087	2.3(-4)	4.5(-5)	4.5(-5)	4.2(-5)	1.7(-4)	0.003	0.091	0.92	0.167	0.01	0.004
[O I]	6300+	0.025	1.0	2.	3.	2.9	1.36	0.24	0.0	0.0	0.0	0.0
[Fe X]	6374	0.0	0.0	0.0	7.3(-10)	7.4(-9)	3.3(-6)	0.001	0.26	0.66	0.49	0.3
[N II]	6548+	0.46	1.21	4.9	7.43	6.17	2.73	0.6	0.001	2.3(-4)	0.0	0.0
[S II]	6716	0.145	1.79	3.86	5.2	4.79	3.5	2.38	2.5(-5)	0.0	0.0	0.0
[S II]	6731	0.138	1.41	3.12	4.34	4.3	3.47	2.43	2.5(-5)	0.0	0.0	0.0
[O II]	7325	0.34	0.085	0.12	0.13	0.09	0.05	0.026	0.002	3.4(-4)	0.0	0.0
[Fe XI]	7892	0.0	0.0	0.0	0.0	0.0	8.6(-8)	1.8(-4)	0.12	0.51	0.59	0.37
Hβ	erg cm^{-2}s^{-1}	8.11(-4)	0.0043	0.006	0.0126	0.036	0.118	0.33	0.24	0.2	0.16	0.11
[S III]	9532+	0.145	0.67	1.38	1.77	1.76	1.37	1.86	0.026	8.4(-4)	4(-6)	0.0
[C I]	9850	0.033	0.0086	3(-4)	2.6(-4)	1.3(-4)	3.6(-5)	6.5(-6)	0.0	0.0	0.0	0.0
[S VIII]	9913	0.0	1.9(-8)	1.3(-7)	2.2(-7)	9(-7)	1.4(-5)	9.4(-4)	0.24	0.47	0.28	0.04
[S IX]	1.25	0.0	1.4(-10)	1.73(-9)	5.4(-9)	1.7(-8)	9.7(-7)	7.87(-5)	0.045	0.18	0.22	0.08
[Si VI]	1.96	3.7(-6)	1.79(-6)	1.48(-5)	1.2(-4)	0.001	0.005	0.037	0.45	0.055	0.0043	2.5(-4)
[Si VII]	2.48	0.0	8.45(-8)	5.7(-7)	9(-7)	9(-6)	1.5(-4)	0.005	0.35	0.25	0.06	0.008
[Si IX]	2.59	0.0	0.0	0.0	1.6(-9)	1.3(-8)	1.65(-6)	3.3(-4)	0.39	2.76	3.5	2.5
[Mg VIII]	3.03	0.0	0.0	0.0	0.0	3.4(-9)	3.2(-6)	6.7(-4)	0.21	1.12	1.	0.7
[Si IX]	3.9	0.0	0.0	0.0	3.2(-9)	2.5(-8)	4.2(-6)	8(-4)	0.84	5.8	7.2	5.
[Mg VII]	5.5	0.0	7.6(-10)	1.4(-8)	4.2(-8)	9.3(-7)	6.2(-5)	0.0056	0.54	1.	0.37	0.12
[Mg V]	5.6	6.5(-5)	1.3(-5)	1.27(-5)	2.2(-5)	3.22(-4)	0.0044	0.078	0.57	0.03	7(-4)	4(-5)
[Ne VI]	7.6	4.11(-7)	1.57(-7)	4.4(-6)	2.1(-4)	0.007	0.072	0.55	4.4	7.	6.5	3.4
[Ar III]	8.99	0.0056	0.077	0.074	0.073	0.084	0.12	0.18	1(-4)	4(-6)	4(-11)	0.0
[S IV]	10.54	0.02	0.004	0.003	0.005	0.039	0.22	1.33	0.5	0.016	3.5(-4)	0.0
[Ne II]	12.8	1.43	2.5	2.17	1.24	0.36	0.066	0.006	1.2(-4)	1.7(-6)	0.0	0.0
[Ne V]	14.32	1.9(-4)	3.65(-5)	7.5(-4)	0.02	0.26	0.88	1.72	3.11	2.7	1	0.2
[Ne III]	15.55	0.23	0.99	2.27	2.82	2.53	1.9	1.5	0.5	0.013	6.5(-5)	2.4(-6)
[S III]	18.7	0.013	1.84	1.5	1.01	0.58	0.35	0.39	0.0028	8.6(-5)	3(-7)	0.0
[Ne V]	24.3	2.5(-4)	4.8(-5)	7.2(-4)	0.019	0.25	0.86	1.76	3.4	3.	1.14	0.26
[O IV]	25.9	0.07	0.0132	0.048	0.57	2.56	4.	4.7	6.78	3.42	0.37	0.08
[Fe II]	26.	18.3	7.7	5.47	3.0	1.2	0.42	0.08	0.0	0.0	0.0	0.0
[S III]	33.5	0.018	3.5	2.77	1.79	0.97	0.51	0.44	0.0033	1(-4)	4(-7)	0.0
[Si II]	34.86	98.	39.4	26.	13.4	4.8	1.59	0.38	1.6(-4)	0.0	0.0	0.0
[Ne III]	36.01	0.013	0.084	0.2	0.24	0.22	0.167	0.13	0.046	0.0012	6(-6)	2(-7)
[O III]	51.81	0.024	0.0073	0.45	1.67	2.87	3.21	3.3	1.46	0.13	8(-4)	1(-4)
[O I]	63.18	17.	16.3	13.2	8.06	3.36	1.	0.12	0.0	0.0	0.0	0.0
[O III]	88.36	0.022	0.006	0.22	0.81	1.42	1.6	1.73	0.84	0.08	5(-4)	7(-5)
[O I]	145.5	1.1	1.44	1.18	0.73	0.31	0.09	0.01	0.0	0.0	0.0	0.0
[C II]	157.7	12.7	7.68	5.1	2.56	0.83	0.2	0.02	9.2(-6)	2.8(-6)	1.4(-7)	0.0

Table 3

The models : V_s=200 $\mathrm{km\,s^{-1}}$, n_0=200 $\mathrm{cm^{-3}}$, D= 10^{18}cm

		20	21	22	23	24	25	26	27	28	29
log F_h		SD	9	9.48	10	10.78	10.9	11	11.48	11.78	12
O VI	1033	733.	3.5	2.1	0.17	0.057	0.059	0.063	0.16	3.6	21.6
Si III	1206	19.7	0.079	0.045	0.0023	0.0016	0.005	0.026	0.23	0.075	0.0045
H I	1216	145.	24.5	25.1	27.37	25.5	25.5	25.4	25.3	25.93	26.9
N V	1240	43.	0.2	0.123	0.01	0.002	0.002	0.004	0.176	2.	6.86
S II	1256	1.89	0.004	0.0023	2(-4)	0.0014	0.0035	0.014	5(-5)	9(-6)	0.0
Si II	1264	0.5	0.0014	9.5(-4)	1(-4)	2.4(-4)	3.2(-4)	0.0013	0.005	8.5(-4)	4(-5)
O I	1302+	0.05	1.8(-4)	2.6(-4)	6.5(-5)	1(-5)	5(-7)	2.6(-4)	0.0	0.0	0.0
Si IV	1397	12.23	0.057	0.034	0.0023	1.5(-4)	5(-4)	0.0029	0.37	0.7	0.065
O IV	1401+	80.	0.4	0.2	0.018	0.004	0.0035	0.02	0.5	2.8	6.
N IV]	1486	23.	0.08	0.07	0.0054	0.0024	0.006	0.028	0.52	2.6	4.6
C IV	1550	106.	0.52	0.32	0.025	0.025	0.072	0.34	5.0	19.5	32.8
He II	1640	1.3	0.054	0.11	0.025	0.1	0.16	3.04	1.	3.8	7.5
Si III	1892+	16.8	0.05	0.029	0.0028	0.052	0.15	.55	1.7	0.28	1.2(-4)
[Ne V]	3426	7.55	0.036	0.022	0.0017	0.0033	0.0084	0.028	0.5	2.9	6.5
[O II]	3727	42.	0.6	0.9	0.23	0.94	1.3	0.22	0.15	0.063	0.014
[Ne III]	3869+	3.24	0.07	0.12	0.039	0.12	0.22	0.8	1.7	1.65	0.51
[S II]	4073+	0.9	0.066	0.09	0.03	0.14	0.23	0.43	0.01	1(-5)	0.0
[O III]	4363	2.	0.0095	0.006	9.4(-4)	0.009	0.022	0.088	0.29	0.5	0.29
He II	4686	0.095	0.008	0.017	0.0037	0.016	0.024	0.47	0.138	0.5	0.98
[O III]	5007+	24.7	0.126	0.19	0.15	1.86	4.	15.6	30.6	34.0	13.2
[N I]	5200+	0.08	0.014	0.045	0.01	2(-4)	1(-4)	1.6(-6)	5(-7)	0.0	0.0
He I	5876	0.18	0.23	0.16	0.026	0.16	0.15	0.09	0.124	0.075	0.011
[Fe VII]	6087	1.67	0.008	0.005	4(-4)	2.6(-4)	6.4(-4)	0.0027	0.06	0.52	0.61
[O I]	6300+	0.47	1.12	0.87	0.1	0.007	5(-4)	5(-5)	0.0	0.0	0.0
[Fe X]	6374	0.0019	1(-5)	6(-6)	5(-7)	3.5(-7)	6(-7)	2.4(-6)	3.3(-4)	0.022	0.29
[N II]	6548+	6.86	2.07	1.88	0.28	1.13	1.27	0.078	0.055	0.01	0.002
[S II]	6716	1.24	0.97	0.73	0.085	0.35	0.48	0.75	0.0043	1(-5)	0.0
[S II]	6731	1.92	0.99	0.82	0.115	0.62	0.83	1.3	0.0075	1.9(-5)	0.0
[O II]	7325	6.7	0.034	0.048	0.012	0.036	0.054	0.017	0.013	0.007	0.002
[Fe XI]	7892	6(-6)	0.0	5(-8)	0.0	0.0	0.0	0.0	4(-5)	0.005	0.11
Hβ	$\mathrm{erg\,cm^{-2}s^{-1}}$	2.2(-4)	0.046	0.075	0.94	2.65	2.45	2.11	1.64	1.25	0.99
[S III]	9532+	2.13	2.95	1.86	0.127	0.3	0.43	0.76	0.55	0.016	0.002
[C I]	9850	0.57	2(-4)	1.8(-4)	3.5(-4)	4.5(-5)	2.6(-5)	0.0	0.0	0.0	0.0
[S VIII]	9913	0.009	4.5(-5)	2.9(-5)	3(-6)	2.8(-6)	5(-6)	1.7(-5)	0.0014	0.08	0.3
[S IX]	1.25	6(-5)	4.(-7)	4(-7)	7.5(-8)	1.4(-7)	2(-7)	7.6(-7)	7.2(-5)	0.006	0.05
[Si VI]	1.96	0.36	0.0017	0.001	8.7(-5)	6.7(-4)	0.0015	0.0034	0.029	0.36	0.96
[Si VII]	2.48	0.18	8.7(-4)	5(-4)	4.3(-5)	2.3(-5)	4(-5)	1.3(-4)	0.004	0.18	0.46
[Si IX]	2.59	2(-4)	1.3(-6)	1.2(-6)	2(-7)	3.5(-7)	5(-7)	8(-7)	1.4(-4)	0.05	0.7
[Mg VIII]	3.03	0.03	1.5(-4)	9(-5)	7.5(-6)	2.9(-6)	3.3(-6)	6(-6)	2.2(-4)	0.027	0.48
[Si IX]	3.9	3.7(-4)	2.4(-6)	2(-6)	3.7(-7)	6.6(-7)	1(-6)	1.5(-6)	3.4(-4)	0.1	1.56
[Mg VII]	5.5	0.26	0.00125	7.6(-4)	6.2(-5)	2.5(-5)	3.5(-5)	8(-5)	0.0027	0.14	1.11
[Mg V]	5.6	0.19	9(-4)	5.5(-4)	4.5(-5)	0.001	0.0024	0.007	0.08	0.47	0.19
[Ne VI]	7.6	1.46	0.007	0.0043	3.4(-4)	7(-4)	0.002	0.006	0.165	1.3	3.9
[Ar III]	8.99	0.085	0.43	0.31	0.045	0.14	0.16	0.18	0.04	0.001	2(-5)
[S IV]	10.54	0.29	0.0024	0.0016	2.7(-4)	0.085	0.17	0.4	2.94	0.47	0.06
[Ne II]	12.8	0.5	1.37	0.92	0.093	0.39	0.38	0.085	0.005	7.6(-4)	6(-5)
[Ne V]	14.32	0.4	0.0019	0.0012	1.5(-4)	0.018	0.045	0.14	0.93	3.25	4.9
[Ne III]	15.55	0.43	0.57	0.58	0.11	0.25	0.34	1.34	1.5	0.8	0.14
[S III]	18.7	0.2	3.78	2.43	0.19	0.13	0.16	0.21	0.11	0.0023	2(-4)
[Ne V]	24.3	0.56	0.0026	0.0016	1.6(-4)	0.011	0.028	0.086	0.64	2.37	3.75
[O IV]	25.9	2.2	0.01	0.0065	0.0018	0.18	0.33	2.4	2.48	6.	6.32
[Fe II]	26.	1.	4.0	2.86	0.6	0.082	0.035	0.011	1(-5)	0.0	0.0
[S III]	33.5	0.12	4.37	2.65	0.14	0.046	0.056	0.075	0.044	0.001	1(-4)
[Si II]	34.86	2.98	11.0	7.16	0.75	0.16	0.1	0.05	0.013	2.5(-4)	4(-6)
[Ne III]	36.01	0.036	0.048	0.048	0.009	0.02	0.027	0.1	0.12	0.065	0.012
[O III]	51.81	0.27	0.003	0.016	0.015	0.19	0.4	1.39	1.66	1.15	0.3
[O I]	63.18	1.1	6.65	4.11	0.3	0.0016	1.7(-4)	2(-6)	0.0	0.0	0.0
[O III]	88.36	0.09	8.7(-4)	0.003	0.0028	0.034	0.07	0.24	0.3	0.22	0.058
[O I]	145.5	0.076	0.46	0.28	0.019	6(-5)	7(-6)	0.0	0.0	0.0	0.0
[C II]	157.7	0.125	0.5	0.3	0.024	0.0017	0.001	2(-4)	8(-5)	2(-5)	3(-6)

Table 4
The models : V_s=200 $km\,s^{-1}$, n_0=200 cm^{-3}, D= 10^{19}cm

		30	31	32	33	34	35	36	37	38	39
log F_h		SD	9	9.48	10	10.48	11	11.48	11.78	12	12.48
O VI	1033	733.	3.37	0.39	0.16	0.007	0.0053	0.0067	0.06	0.32	21.1
Si III	1206	19.7	0.076	0.0086	0.003	9(-5)	3.6(-4)	0.008	0.086	0.26	0.06
H I	1216	145.	24.68	24.2	24.9	28.	25.8	25.4	25.3	25.3	25.8
N V	1240	43.	0.19	0.022	0.0094	4(-4)	3.2(-4)	0.003	0.046	0.15	3.
S II	1256	1.89	0.004	5(-4)	3(-4)	4.49-5)	2.8(-4)	0.0044	0.035	0.077	1(-4)
Si II	1264	0.47	0.00157	1.9(-4)	1.4(-4)	1.6(-5)	5.3(-5)	3.4(-4)	0.002	0.007	5(-4)
O I	1302+	0.048	5.6(-4)	6(-5)	7(-5)	1(-5)	4(-5)	2.7(-5)	3.6(-5)	3.7(-5)	0.0
Si IV	1397	12.2	0.054	0.006	0.0025	8(-5)	2.7(-5)	7.8(-4)	0.01	0.032	1.12
O IV	1401+	79.	0.36	0.04	0.016	7(-4)	7.5(-4)	0.01	0.1	0.19	1.7
N IV]	1486	23.	0.11	0.012	5.1(-3)	2.5(-4)	6.5(-4)	0.013	0.13	0.25	2.1
C IV	1550	106.	0.5	0.058	0.024	0.0013	0.006	0.13	1.08	2.38	17.7
He II	1640	1.3	0.128	0.025	0.033	0.0044	0.011	1.28	4.3	4.1	2.13
Si III	1892+	16.77	0.049	0.0058	0.0042	0.0012	0.008	0.13	0.7	1.53	0.1
[Ne V]	3426	7.55	0.034	0.004	0.0017	9(-5)	6.7(-4)	0.02	0.12	0.26	1.8
[O II]	3727	42.	2.2	0.4	0.34	0.024	0.2	0.34	0.043	0.087	0.017
[Ne III]	3869+	3.24	0.39	0.045	0.053	0.0068	0.023	0.18	0.67	1.29	2.35
[S II]	4073+	0.9	0.35	0.06	0.043	0.004	0.033	0.15	0.32	0.4	2.4(-5)
[O III]	4363	2.	0.009	0.0011	0.0011	3(-4)	0.0015	0.016	0.062	0.15	0.53
He II	4686	0.095	0.02	0.0038	0.005	6.7(-4)	0.0016	0.2	0.67	0.62	0.26
[O III]	5007+	24.7	0.12	0.035	0.19	0.065	0.31	4.7	10.8	21.2	41.2
[N I]	5200+	0.083	3.	0.28	0.11	2.3(-4)	4(-4)	1(-5)	0.0	0.0	0.0
He I	5876	0.18	0.43	0.24	0.12	0.012	0.17	0.13	0.067	0.07	0.11
[Fe VII]	6087	1.67	0.008	9(-4)	3.7(-4)	1.6(-5)	2.2(-5)	9(-4)	0.01	0.035	0.56
[O I]	6300+	0.47	9.4	1.27	0.57	0.013	0.025	7(-5)	5(-6)	5(-6)	0.0
[Fe X]	6374	0.002	9(-6)	1(-6)	5(-7)	2.4(-8)	3(-8)	1(-6)	6(-5)	3(-4)	0.049
[N II]	6548+	6.86	2.67	1.14	0.74	0.035	0.5	0.25	0.02	0.036	8(-4)
[S II]	6716	1.24	4.89	1.05	0.45	0.012	0.13	0.37	0.59	0.63	2.3(-5)
[S II]	6731	1.92	4.5	1.04	0.47	0.015	0.23	0.63	1.	1.1	3.8(-5)
[O II]	7325	6.7	0.057	0.015	0.015	0.0018	0.005	0.016	0.0024	0.006	0.0018
[Fe XI]	7892	5.6(-6)	3.5(-8)	0.0	0.0	0.0	0.0	7(-8)	1(-5)	4(-5)	0.017
Hβ	$erg\,cm^{-2}s^{-1}$	2.2(-4)	0.048	0.42	0.99	22.5	29.3	21.9	18.25	18.7	11.5
[S III]	9532+	2.13	15.3	3.3	1.18	0.017	0.13	0.36	0.71	1.46	0.045
[C I]	9850	0.57	0.27	9(-4)	4(-4)	5(-6)	5(-5)	2.4(-5)	0.0	0.0	0.0
[S VIII]	9913	0.0088	4(-5)	5(-6)	2.3(-6)	1.2(-7)	3.7(-7)	1.7(-5)	2(-4)	7.4(-4)	0.035
[S IX]	1.25	5.9(-5)	4(-7)	7(-8)	7(-8)	0.0	2(-8)	1.5(-6)	2.2(-5)	8.6(-5)	0.007
[Si VI]	1.96	0.36	0.0017	2(-4)	8(-5)	5(-6)	4(-4)	0.005	0.019	0.043	0.25
[Si VII]	2.48	0.18	8(-4)	1(-4)	4(-5)	1.8(-6)	6(-6)	2(-4)	0.0017	0.0054	0.15
[Si IX]	2.59	2(-4)	1.2(-6)	2(-7)	2(-7)	2(-8)	5(-8)	5(-6)	1.2(-4)	5(-4)	0.077
[Mg VIII]	3.03	0.03	1.4(-4)	1.6(-5)	7(-6)	3.2(-7)	3(-7)	2.3(-5)	5(-4)	0.0019	0.11
[Si IX]	3.9	3.7(-4)	2.3(-6)	4(-7)	3(-7)	4(-8)	9(-8)	1.5(-5)	3.3(-4)	0.0013	0.17
[Mg VII]	5.5	0.26	0.0012	1.4(-4)	6(-5)	2.6(-6)	5(-6)	3(-4)	0.0037	0.013	0.29
[Mg V]	5.6	0.19	8.7(-4)	1(-4)	4.6(-5)	3.2(-6)	8(-4)	0.013	0.057	0.13	0.45
[Ne VI]	7.6	1.46	0.0067	7.8(-4)	3.3(-4)	1.8(-5)	1.6(-4)	0.009	0.06	0.16	1.68
[Ar III]	8.99	0.085	0.87	0.47	0.24	0.019	0.1	0.14	0.17	0.18	0.0023
[S IV]	10.54	0.29	0.0036	0.0013	7(-4)	1.2(-4)	0.029	0.21	0.54	0.93	1.27
[Ne II]	12.8	0.52	3.7	1.48	0.7	0.039	0.39	0.21	0.045	0.02	2.5(-4)
[Ne V]	14.32	0.41	0.0018	2(-4)	1.9(-4)	1.9(-4)	0.0033	0.1	0.34	0.54	1.55
[Ne III]	15.55	0.43	2.85	0.56	0.38	0.028	0.086	0.79	1.38	1.54	1.17
[S III]	18.7	0.2	8.03	4.2	1.9	0.068	0.1	0.15	0.2	0.33	0.0047
[Ne V]	24.3	0.56	0.0025	2.9(-4)	1.8(-4)	1.2(-4)	0.002	0.06	0.22	0.35	1.15
[O IV]	25.9	2.2	0.01	0.0012	0.0029	0.002	0.0029	0.87	4.1	3.67	2.64
[Fe II]	26.	1.05	7.58	4.44	2.47	0.39	0.18	0.03	0.01	0.003	0.0
[S III]	33.5	0.12	10.3	4.86	1.97	0.039	0.037	0.055	0.076	0.12	0.0023
[Si II]	34.86	2.98	22.2	12.2	5.8	0.34	0.23	0.095	0.05	0.031	2.2(-5)
[Ne III]	36.01	0.036	0.25	0.05	0.03	0.0021	0.007	0.061	0.11	0.12	0.1
[O III]	51.81	0.27	0.003	0.0032	0.019	0.0056	0.038	1.14	1.16	1.38	1.5
[O I]	63.18	1.1	18.	7.39	3.08	0.1	0.018	1.5(-5)	5(-8)	5(-8)	0.0
[O III]	88.36	0.09	0.0011	7.5(-4)	0.0035	0.001	0.0066	0.2	0.2	0.25	0.29
[O I]	145.5	0.076	1.27	0.52	0.21	0.006	0.0011	6(-7)	0.0	0.0	0.0
[C II]	157.7	0.12	1.19	0.55	0.23	0.01	0.0035	5.7(-4)	9(-5)	8.5(-5)	2(-6)

Table 5

The models : V_s=100 $\mathrm{km\,s^{-1}}$, n_0=300 $\mathrm{cm^{-3}}$, D= 10^{17}cm

		40	41	42	43	44	45	46	47
log F_h		SD	8	9	10	10.48	11	11.48	12
O VI	1033	0.01	0.0016	0.0024	0.0015	0.0016	0.049	4.87	55.
Si III	1206	24.7	2.84	1.13	0.066	0.022	0.044	0.01	1.6(-4)
H I	1216	151.3	38.	32.73	32.5	25.28	25.6	26.93	27.8
N V	1240	2.3	0.266	0.11	0.009	0.0049	0.14	3.88	10.1
S II	1256	2.28	0.26	0.107	0.014	0.0029	2.7(-4)	1.6(-7)	0.0
Si II	1264	0.56	0.065	0.027	0.006	0.0019	7.3(-4)	1.1(-4)	0.0
O I	1302+	0.056	0.007	0.0042	0.0035	5.2(-5)	3.3(-6)	0.0	0.0
Si IV	1397	15.3	1.76	0.7	0.038	0.0195	0.25	0.1	0.0026
O IV	1401+	22.4	2.7	1.07	0.075	0.04	0.75	8.	3.7
N IV]	1486	15.	1.9	0.68	0.05	0.04	0.7	4.1	2.5
C IV	1550	103.4	11.9	4.8	0.34	0.284	6.75	27.3	18.6
He II	1640	0.25	0.54	0.72	0.98	1.14	4.78	7.69	8.14
Si III	1892+	21.	2.4	0.97	0.15	0.39	0.45	0.039	3.(-4)
[Ne V]	3426	0.02	0.0023	0.001	5.(-4)	0.013	0.87	6.13	7.2
[O II]	3727	58.	8.5	7.5	7.	2.3	0.35	0.017	1.9(-4)
[Ne III]	3869+	2.84	0.7	0.88	1.21	1.128	1.65	0.24	0.01
[S II]	4073+	1.0	0.62	0.66	0.62	0.1	5.(-4)	4.(-9)	0.0
[O III]	4363	2.16	0.25	0.1	0.031	0.099	0.4	0.165	0.011
He II	4686	0.022	0.085	0.11	0.15	0.17	0.68	1.03	1.0
[O III]	5007+	27.	3.11	1.47	6.42	17.75	33.24	6.79	0.29
[N I]	5200+	0.098	1.36	0.55	0.031	0.008	7.(-6)	0.0	0.0
He I	5876	0.146	0.58	0.27	0.15	0.123	0.056	0.006	0.0012
[Fe VII]	6087	0.0023	2.8(-4)	1.8(-4)	9.(-5)	0.0016	0.32	0.86	0.093
[O I]	6300+	0.45	5.18	3.33	1.46	0.033	6.5(-5)	0.0	0.0
[Fe X]	6374	0.0	0.0	0.0	5.(-9)	3.9(-7)	0.0013	0.11	0.65
[N II]	6548+	8.3	4.36	6.73	5.79	1.44	0.124	0.008	1.4(-4)
[S II]	6716	1.48	6.09	3.55	1.65	0.21	8.(-4)	9.(-9)	0.0
[S II]	6731	2.18	6.29	4.03	2.43	0.34	0.0013	9.4(-9)	0.0
[O II]	7325	7.95	0.95	0.55	0.39	0.135	0.034	0.0023	3.(-5)
[Fe XI]	7892	0.0	0.0	0.0	0.0	2.(-9)	1.37(-4)	0.025	0.41
Hβ	$\mathrm{erg\,cm^{-2}s^{-1}}$	1.5(-4)	0.0013	0.0032	0.045	0.133	0.11	0.077	0.059
[S III]	9532+	2.74	1.68	1.53	1.6	3.12	0.24	0.0032	8.5(-5)
[C I]	9850	0.53	0.011	0.0094	0.003	7.9(-4)	5.5(-5)	0.0	0.0
[S VIII]	9913	0.0	6.9(-8)	5.6(-7)	2.9(-6)	3.4(-5)	0.012	0.177	0.45
[S IX]	1.25	0.0	0.0	3.2(-9)	4.7(-8)	5.9(-7)	3.5(-4)	0.014	0.133
[Si VI]	1.96	2.9(-5)	3.3(-5)	1.2(-4)	1.75(-4)	0.0034	0.276	0.41	0.063
[Si VII]	2.48	0.0	2.2(-7)	1.4(-6)	8.(-6)	1.87(-4)	0.07	0.44	0.29
[Si IX]	2.59	0.0	0.0	0.0	3.3(-8)	5.4(-7)	0.0024	0.194	2.187
[Mg VIII]	3.03	0.0	0.0	0.0	2.6(-9)	1.1(-7)	0.0045	0.22	1.07
[Si IX]	3.9	0.0	0.0	0.0	6.3(-8)	1.06(-6)	0.0059	0.44	4.67
[Mg VII]	5.5	0.0	0.0	7.2(-9)	1.3(-7)	8.9(-6)	0.063	0.93	1.1
[Mg V]	5.6	5.7(-4)	6.8(-5)	3.8(-5)	4.7(-5)	0.0016	0.474	0.28	0.015
[Ne VI]	7.6	2.7(-6)	5.7(-7)	1.2(-6)	5.5(-5)	0.0019	0.186	2.3	6.65
[Ar III]	8.99	0.1	0.086	0.07	0.14	0.37	0.033	6.2(-5)	0.0
[S IV]	10.54	0.35	0.04	0.017	0.046	0.77	1.49	0.082	0.0027
[Ne II]	12.8	0.296	2.3	1.05	0.14	0.034	0.0033	4.(-5)	0.0
[Ne V]	14.32	0.0017	2.(-4)	1.(-4)	0.0056	0.087	2.27	6.47	3.75
[Ne III]	15.55	0.19	2.57	2.4	1.9	1.58	0.88	0.057	0.0015
[S III]	18.7	0.26	1.194	0.95	0.44	0.83	0.043	4.2(-4)	9.2(-6)
[Ne V]	24.3	0.0022	2.6(-4)	1.2(-4)	0.0035	0.057	1.6	5.	3.19
[O IV]	25.9	0.85	0.098	0.04	0.15	0.89	8.3	9.94	1.69
[Fe II]	26.	0.69	5.27	2.53	0.62	0.096	2.7(-6)	0.0	0.0
[S III]	33.5	0.19	1.68	1.39	0.34	0.35	0.019	2.(-4)	4.8(-6)
[Si II]	34.86	1.77	15.76	7.7	0.98	0.228	0.0026	3.7(-5)	0.0
[Ne III]	36.01	0.017	0.22	0.2	0.155	0.127	0.072	0.0048	1.25(-4)
[O III]	51.81	0.35	0.041	0.053	0.65	1.44	1.37	0.153	0.0047
[O I]	63.18	0.42	11.54	0.6	0.55	0.008	5.8(-6)	0.0	0.0
[O III]	88.36	0.16	0.0187	0.015	0.126	0.28	0.27	0.032	0.001
[O I]	145.5	0.028	0.84	0.45	0.035	3.5(-4)	2.2(-7)	0.0	0.0
[C II]	157.7	0.04	1.10	0.59	0.032	0.0026	2.8(-4)	1.5(-5)	4.8(-7)

Table 6

The models : V_s=100 $km\,s^{-1}$, n_0=300 cm^{-3}, D= 10^{19}cm

		48	49	50	51	52	53	54	55
log F_h		SD	8	9	10	10.48	11	11.48	12
O VI	1033	0.01	1.6(-5)	8.5(-5)	1.3(-4)	1.7(-4)	0.0012	0.03	0.83
Si III	1206	24.7	0.039	0.15	0.063	0.035	0.045	0.13	0.55
H I	1216	151.3	24.6	38.	46.	49.5	46.9	46.6	25.56
N V	1240	2.3	0.0037	0.014	0.006	0.003	0.007	0.06	0.32
S II	1256	2.3	0.004	0.021	0.019	0.022	0.039	0.087	0.023
Si II	1264	0.56	0.001	0.0073	0.008	0.009	0.009	0.01	0.016
O I	1302+	0.056	5.4(-4)	0.0074	0.01	0.012	0.01	0.0095	2.5(-4)
Si IV	1397	15.3	0.024	0.093	0.038	0.018	0.007	0.012	0.068
O IV	1401+	22.3	0.035	0.14	0.055	0.05	0.055	0.18	0.35
N IV]	1486	15.	0.02	0.095	0.04	0.025	0.065	0.22	0.45
C IV	1550	103.4	0.164	0.63	0.266	0.2	0.73	2.26	3.66
He II	1640	0.25	0.71	1.34	0.72	1.04	1.3	1.29	0.52
Si III	1892+	21.	0.033	0.13	0.11	0.3	0.87	1.75	2.3
[Ne V]	3426	0.02	3.2(-5)	1.2(-4)	3.2(-4)	0.0078	0.1	0.37	0.45
[O II]	3727	58.	2.4	4.1	4.4	3.67	2.3	1.44	0.82
[Ne III]	3869+	2.84	0.53	3.05	2.	2.09	2.3	2.	1.36
[S II]	4073+	1.	0.7	1.8	1.08	1.1	0.12	1.	0.07
[O III]	4363	2.16	0.0034	0.013	0.02	0.064	0.13	0.18	0.18
He II	4686	0.022	0.11	0.21	0.11	0.156	0.19	0.18	0.07
[O III]	5007+	27.	0.044	0.19	4.25	13.	21.5	24.4	22.6
[N I]	5200+	0.098	1.94	7.8	2.46	0.87	0.23	0.023	2.(-4)
He I	5876	0.146	0.75	1.2	0.45	0.22	0.14	0.12	0.14
[Fe VII]	6087	.0023	3.7(-6)	1.5(-6)	1.3(-5)	2.(-5)	2.5(-4)	0.004	0.048
[O I]	6300+	0.45	7.05	23.4	10.9	7.32	5.47	2.47	0.27
[Fe X]	6374	0.0	0.0	0.0	0.0	5.(-10)	3.6(-9)	5.5(-6)	6.2(-4)
[N II]	6548+	8.3	3.62	6.53	9.93	10.38	8.78	4.	0.88
[S II]	6716	1.48	8.06	21.5	8.75	6.48	4.3	2.4	0.133
[S II]	6731	2.18	8.11	18.56	7.77	6.27	4.87	3.4	0.21
[O II]	7325	7.95	0.06	0.146	0.2	0.19	0.12	0.066	0.034
[Fe XI]	7892	0.0	0.0	0.0	0.0	0.0	0.0	3.5(-7)	1.(-4)
Hβ	$erg\,cm^{-2}s^{-1}$	1.5(-4)	0.093	0.024	0.058	0.124	0.38	1.356	10.57
[S III]	9532+	2.74	1.68	6.65	3.74	4.06	3.7	2.27	3.87
[C I]	9850	0.53	0.23	0.022	0.011	0.004	8.(-4)	1.6(-4)	4.(-5)
[S VIII]	9913	0.0	5(-10)	1.8(-8)	8.(-8)	1.5(-7)	3.4(-6)	6.(-5)	0.001
[S IX]	1.25	0.0	0.0	7.6(-11)	1.5(-9)	5.5(-9)	2.4(-7)	5.(-6)	1.5(-4)
[Si VI]	1.96	2.9(-5)	7.5(-8)	1.6(-6)	4.4(-5)	4.(-4)	0.003	0.012	0.039
[Si VII]	2.48	0.0	2.85(-9)	1.1(-7)	4.7(-7)	1.7(-6)	3.8(-5)	5.4(-4)	0.006
[Si IX]	2.59	0.0	0.0	0.0	0.0	5.4(-9)	2.5(-8)	1.8(-5)	8.(-4)
[Mg VIII]	3.03	0.0	0.0	0.0	0.0	1.(-9)	8.8(-9)	4.(-5)	0.0023
[Si IX]	3.9	0.0	0.0	0.0	0.0	1.(-8)	4.8(-8)	4.5(-5)	0.002
[Mg VII]	5.5	0.0	0.0	7.4(-10)	1.5(-8)	5.7(-8)	1.2(-5)	5.(-4)	0.014
[Mg V]	5.6	5.7(-4)	9.2(-7)	4.2(-6)	6.8(-6)	7.4(-5)	0.0013	0.015	0.1
[Ne VI]	7.6	2.7(-6)	5.5(-9)	6.8(-8)	3.8(-5)	0.0014	0.033	0.19	0.3
[Ar III]	8.99	0.1	0.097	0.17	0.09	0.083	0.09	0.12	0.3
[S IV]	10.54	0.35	5.5(-4)	0.002	0.0017	0.0073	0.059	0.25	0.76
[Ne II]	12.8	0.296	2.87	4.73	2.78	1.59	0.38	0.068	0.018
[Ne V]	14.32	0.0017	2.7(-6)	1.3(-5)	0.004	0.07	0.52	1.08	0.65
[Ne III]	15.55	0.19	3.49	10.6	5.26	4.66	3.22	2.1	1.67
[S III]	18.7	0.26	1.51	4.58	2.97	2.11	1.09	0.53	0.97
[Ne V]	24.3	0.0022	3.5(-6)	1.5(-5)	0.0025	0.045	0.35	0.76	0.48
[O IV]	25.9	0.85	0.0013	0.005	0.1	0.73	2.1	2.5	1.12
[Fe II]	26.	0.69	7.	16.3	8.3	4.12	1.47	0.52	0.128
[S III]	33.5	0.19	2.17	7.72	5.07	3.37	1.64	0.67	0.45
[Si II]	34.86	1.77	21.5	63.7	34.5	15.5	4.93	1.47	0.24
[Ne III]	36.01	0.017	0.3	0.92	0.45	0.4	0.27	0.176	0.135
[O III]	51.81	0.35	0.0014	0.008	0.44	1.1	1.52	1.55	1.69
[O I]	63.18	0.42	15.7	44.5	25.56	16.8	6.7	1.91	0.08
[O III]	88.36	0.16	7.(-4)	0.0027	0.086	0.21	0.3	0.3	0.33
[O I]	145.5	0.028	1.15	3.33	1.94	1.29	0.51	0.14	0.004
[C II]	157.7	0.04	1.36	5.74	3.19	1.5	0.48	0.12	0.0033

Table 7
The models : V_s=300 $km\,s^{-1}$, n_0=300 cm^{-3}, D= 10^{17}cm

		56	57	58	59	60	61	62
log F_h		SD	8	9	10	10.48	11	12
O VI	1033	732.	0.74	0.3	0.3	0.26	0.29	2.92
Si III	1206	14.77	2(-4)	1.8(-4)	5.5(-4)	0.0027	0.05	0.04
H I	1216	92.3	27.4	27.5	27.6	27.6	27.6	29.5
N V	1240	36.4	0.026	0.01	0.008	0.006	0.008	2.68
S II	1256	1.37	1.8(-4)	1.5(-4)	3.5(-4)	0.0014	0.017	1(-5)
Si II	1264	0.34	1.9(-5)	1.6(-4)	2.6(-4)	8(-5)	0.001	5(-4)
O I	1302+	0.027	7(-7)	2.6(-7)	2(-7)	1.4(-7)	0.0	0.0
Si IV	1397	8.52	3(-4)	1.4(-4)	1.7(-4)	0.0013	0.011	0.31
O IV	1401+	55.	0.1	0.012	0.006	0.0024	0.038	5.6
N IV]	1486	16.	1.5(-3)	6(-4)	3(-4)	0.001	0.034	4.1
C IV	1550	80.6	0.018	0.007	0.007	0.016	0.43	32.4
He II	1640	2.66	0.33	0.13	0.17	0.25	1.1	6.6
Si III	1892+	12.4	0.04	0.037	0.05	0.1	0.97	0.18
[Ne V]	3426	6.5	7(-3)	0.003	0.006	0.0025	0.022	4.7
[O II]	3727	18.	0.03	0.027	0.018	0.02	0.03	0.046
[Ne III]	3869+	3.05	0.07	0.045	0.08	0.16	1.3	1.12
[S II]	4073+	0.94	0.24	0.24	0.3	0.24	0.56	1.6(-5)
[O III]	4363	1.48	0.013	0.012	0.013	0.022	0.18	0.58
He II	4686	0.20	0.05	0.02	0.027	0.04	0.16	0.89
[O III]	5007+	18.8	8.1	7.77	7.56	8.25	25.8	26.4
[N I]	5200+	0.3	3(-5)	1.4(-5)	9(-6)	5(-6)	0.0	0.0
He I	5876	0.42	0.14	0.15	0.15	0.15	0.13	0.03
[Fe VII]	6087	2.3	2.5(-3)	0.001	0.001	0.0011	0.005	0.89
[O I]	6300+	1.53	7(-4)	2.7(-4)	1.7(-4)	9(-5)	0.0	0.0
[Fe X]	6374	0.68	7.6(-4)	3(-4)	3(-4)	3(-4)	4(-4)	0.05
[N II]	6548+	5.	0.017	0.015	0.013	0.015	0.01	0.017
[S II]	6716	1.64	0.24	0.23	0.22	0.22	0.36	0.0
[S II]	6731	2.49	0.5	0.47	0.45	0.45	0.7	0.0
[O II]	7325	5.7	2.6(-3)	0.0023	0.0016	0.0024	0.005	0.013
[Fe XI]	7892	0.06	6.6(-5)	2.7(-5)	3(-5)	3(-5)	4(-5)	0.011
Hβ	erg $cm^{-2}s^{-1}$	6.8(-4)	0.6	1.5	1.54	1.53	1.18	0.77
[S III]	9532+	1.54	0.73	0.68	0.67	0.7	1.5	0.014
[C I]	9850	3.13	3(-8)	1(-9)	0.0	0.0	0.0	0.0
[S VIII]	9913	0.26	2.8(-4)	1.2(-4)	1.2(-4)	1.3(-4)	2.2(-4)	0.13
[S IX]	1.25	0.1	1(-4)	4.3(-5)	4.3(-5)	4.4(-5)	6.3(-5)	0.009
[Si VI]	1.96	0.4	5(-4)	2.4(-4)	3.3(-4)	5.6(-4)	4(-3)	0.45
[Si VII]	2.48	0.7	7.7(-4)	3(-4)	3(-4)	3(-4)	5.4(-4)	0.35
[Si IX]	2.59	0.57	6.4(-4)	2.6(-4)	2.6(-4)	2.7(-4)	3.9(-4)	0.11
[Mg VIII]	3.03	0.65	7(-4)	2.9(-4)	2.8(-4)	2.8(-4)	3.6(-4)	0.1
[Si IX]	3.9	1.06	1.2(-3)	4.8(-9)	5(-4)	5(-4)	7(-4)	0.24
[Mg VII]	5.5	0.78	8.5(-4)	3.4(-4)	3.4(-4)	3.4(-4)	5(-4)	0.54
[Mg V]	5.6	0.16	0.0037	3(-3)	0.003	0.0043	0.018	0.51
[Ne VI]	7.6	1.4	0.0014	5.8(-4)	6(-4)	5.9(-4)	0.0025	1.58
[Ar III]	8.99	0.065	0.22	0.22	0.21	0.21	0.22	7.4(-4)
[S IV]	10.54	0.18	0.12	0.116	0.14	0.21	0.75	0.21
[Ne II]	12.8	1.33	0.42	0.44	0.41	0.37	0.09	3.4(-4)
[Ne V]	14.32	0.36	5(-4)	2.2(-4)	6(-4)	0.0035	0.07	4.39
[Ne III]	15.55	1.54	0.24	0.17	0.25	0.35	1.3	0.28
[S III]	18.7	0.12	0.18	0.17	0.16	0.17	0.23	0.0013
[Ne V]	24.3	0.46	6(-4)	2.4(-6)	3.5(-4)	0.0014	0.026	2.07
[O IV]	25.9	1.16	0.1	0.047	0.09	0.18	0.86	5.3
[Fe II]	26.	3.63	0.007	0.007	0.0074	0.007	0.002	0.0
[S III]	33.5	0.036	0.036	0.033	0.032	0.033	0.046	2.9(-4)
[Si II]	34.86	9.73	0.025	0.025	0.025	0.025	0.013	7(-5)
[Ne III]	36.01	0.12	0.016	0.011	0.017	0.023	0.09	0.02
[O III]	51.81	0.12	0.7	0.66	0.65	0.64	0.76	0.28
[O I]	63.18	6.38	9(-5)	3.6(-5)	2.4(-5)	1.4(-5)	0.0	0.0
[O III]	88.36	0.02	0.089	0.08	0.08	0.08	0.1	0.037
[O I]	145.5	0.37	3(-6)	1.2(-6)	8.7(-7)	5.4(-7)	0.0	0.0
[C II]	157.7	0.26	1(-5)	8(-6)	8(-6)	1(-5)	5.6(-6)	1(-5)

Table 8
The models : V_s=300 $km\,s^{-1}$, n_0=300 cm^{-3}, D= 10^{19}cm

		63	64	65	66	67	68	69
log F_h		SD	8	9	9.48	10	11	12
O VI	1033	664.	0.08	0.085	0.0045	0.002	0.002	0.0023
Si III	1206	13.4	7(-5)	6.7(-5)	6(-6)	4(-6)	3(-4)	0.0054
H I	1216	86.5	30.11	30.1	27.6	27.7	27.7	27.7
N V	1240	33.	0.003	0.003	1.6(-4)	7(-5)	5(-5)	0.002
S II	1256	1.24	9(-4)	9(-4)	6(-6)	3.4(-6)	2(-4)	0.0023
Si II	1264	0.31	0.003	0.001	8(-7)	4(-7)	2.4(-5)	2.1(-4)
O I	1302+	0.024	0.002	0.0018	0.0	0.0	1(-5)	3(-5)
Si IV	1397	7.73	7(-5)	7(-5)	4(-6)	2(-6)	5.5(-5)	8(-4)
O IV	1401+	51.	0.0033	0.0028	1.8(-4)	6(-5)	4(-4)	0.009
N IV]	1486	14.5	2(-4)	1.7(-4)	8(-6)	3.2(-6)	2.7(-4)	0.008
C IV	1550	73.	0.002	0.0022	1.1(-4)	5.2(-5)	0.0035	0.1
He II	1640	2.4	0.11	0.11	0.0066	0.0038	0.11	1.46
Si III	1892+	11.3	0.017	0.016	0.0027	0.0013	0.023	0.09
[Ne V]	3426	5.85	8(-4)	8(-4)	4.3(-5)	2(-5)	6(-5)	0.009
[O II]	3727	16.8	1.6	1.5	0.086	0.11	0.11	0.14
[Ne III]	3869+	2.7	0.167	0.16	0.004	0.0026	0.047	0.22
[S II]	4073+	0.85	0.7	0.3	0.06	0.052	0.11	0.18
[O III]	4363	1.35	0.006	0.0056	0.0011	5(-4)	0.006	0.014
He II	4686	0.18	0.002	0.017	0.001	6(-4)	0.018	0.23
[O III]	5007+	17.1	4.6	4.5	1.45	0.6	2.8	5.3
[N I]	5200+	0.26	0.57	0.58	1(-6)	3(-6)	0.0	6(-6)
He I	5876	0.56	0.19	0.19	0.17	0.17	0.16	0.12
[Fe VII]	6087	2.11	3(-4)	3(-4)	2(-5)	1(-5)	6(-5)	0.0014
[O I]	6300+	1.39	2.94	3.	6(-6)	1.8(-5)	0.015	0.02
[Fe X]	6374	0.62	9(-5)	8.8(-5)	4(-6)	2(-6)	2(-6)	4(-6)
[N II]	6548+	4.5	1.7	1.74	0.33	0.47	0.32	0.25
[S II]	6716	1.5	0.76	0.76	0.093	0.074	0.12	0.17
[S II]	6731	2.27	1.2	1.2	0.19	0.15	0.25	0.35
[O II]	7325	5.15	0.06	0.06	0.004	0.0044	0.005	0.01
[Fe XI]	7892	0.053	7(-6)	7.6(-6)	4(-7)	2(-7)	2(-7)	4(-7)
Hβ	erg $cm^{-2}s^{-1}$	7.5(-4)	5.4	5.35	102.	217.	216.	194.
[S III]	9532+	1.4	3.9	3.95	0.31	0.25	0.39	0.61
[C I]	9850	2.87	2.5(-5)	2.4(-5)	0.0	5(-8)	1(-7)	2(-6)
[S VIII]	9913	0.23	3.3(-5)	3.3(-5)	2(-6)	8(-7)	1(-6)	2.4(-5)
[S IX]	1.25	0.09	1.2(-5)	1.2(-5)	6(-7)	3(-7)	3(-7)	2.3(-6)
[Si VI]	1.96	0.37	1(-4)	1(-4)	4(-5)	5(-5)	5(-4)	0.006
[Si VII]	2.48	0.63	9(-5)	9(-5)	5(-6)	2.4(-6)	1(-5)	3.3(-4)
[Si IX]	2.59	0.52	7.3(-5)	7.3(-5)	4(-6)	1.8(-6)	2(-6)	1(-5)
[Mg VIII]	3.03	0.59	8.2(-5)	8(-5)	4(-6)	2(-6)	2(-6)	4.33(-5)
[Si IX]	3.9	0.96	1.3(-4)	1.4(-4)	7(-6)	3.4(-6)	4(-6)	2.5(-5)
[Mg VII]	5.5	0.71	1(-4)	1(-4)	5(-6)	2.4(-6)	8(-6)	5.6(-4)
[Mg V]	5.6	0.15	0.0027	2.7(-3)	0.0017	0.0014	0.003	0.026
[Ne VI]	7.6	1.27	1.6(-4)	1.6(-4)	9(-6)	4(-6)	6(-6)	0.0034
[Ar III]	8.99	0.06	0.4	0.4	0.17	0.16	0.17	0.19
[S IV]	10.54	0.17	0.1	0.1	0.08	0.066	0.086	0.24
[Ne II]	12.8	1.39	0.83	0.83	0.42	0.41	0.39	0.21
[Ne V]	14.32	0.32	6(-5)	6(-5)	1.3(-5)	2.3(-5)	6(-4)	0.04
[Ne III]	15.55	1.45	0.46	0.45	0.046	0.04	0.15	0.72
[S III]	18.7	0.1	1.3	1.3	0.13	0.12	0.13	0.16
[Ne V]	24.3	0.4	6(-5)	7(-5)	6(-6)	8(-6)	2(-4)	0.015
[O IV]	25.9	1.06	0.026	0.027	0.0026	0.0024	0.037	0.46
[Fe II]	26.	4.76	0.83	0.84	0.019	0.022	0.023	0.022
[S III]	33.5	0.03	0.66	0.67	0.025	0.022	0.026	0.03
[Si II]	34.86	13.8	1.	1.	0.049	0.053	0.05	0.038
[Ne III]	36.01	0.12	0.036	0.035	0.003	0.0026	0.01	0.05
[O III]	51.81	0.11	0.52	0.52	0.25	0.12	0.26	0.47
[O I]	63.18	7.75	1.1	1.12	2.7(-6)	1.5(-5)	0.005	0.004
[O III]	88.36	0.019	0.07	0.07	0.033	0.016	0.03	0.06
[O I]	145.5	0.44	0.05	0.05	1(-7)	5(-7)	2(-4)	1.5(-4)
[C II]	157.7	0.36	0.03	0.03	1.75(-5)	1.1(-4)	3(-4)	4(-4)

Table 9
The models : V_s=500 $km\,s^{-1}$, n_0=300 cm^{-3}, D= 10^{18}cm

		70	71	72	73	74	75	76
log F_h		SD	8	9	10	11	12	12.7
O VI	1033	130.	0.08	0.088	0.021	0.016	0.01	413.
Si III	1206	2.4	0.0077	0.007	0.0016	6(-5)	0.038	0.51
H I	1216	32.7	29.	29.	29.	29.	29.	29.5
N V	1240	6.05	0.0025	0.0026	6(-4)	4(-4)	0.019	124.
S II	1256	0.22	7(-4)	6(-4)	2(-4)	3.5(-5)	0.0024	0.11
Si II	1264	0.055	2(-4)	1.8(-4)	6(-5)	9(-5)	9(-4)	0.0017
O I	1302+	0.0033	8(-7)	7(-7)	1(-7)	9(-5)	0.0	0.0
Si IV	1397	1.16	0.008	0.0072	0.0024	1.2(-4)	0.029	5.8
O IV	1401+	8.7	6.6	0.058	0.018	1.3(-4)	0.14	740.
N IV]	1486	2.5	5.6	0.05	0.016	3.6(-5)	0.14	310.
C IV	1550	12.55	0.7	0.63	0.22	5.2(-4)	1.55	13.6
He II	1640	2.1	1.17	1.14	6.5	0.017	6.4	4.17
Si III	1892+	2.04	0.18	0.16	0.087	0.0022	0.5	0.36
[Ne V]	3426	1.	0.0026	0.0022	1.8(-4)	2(-4)	0.068	7.9
[O II]	3727	3.2	0.0045	0.004	0.001	0.15	0.0013	0.05
[Ne III]	3869+	1.0	0.54	0.5	0.5	0.022	1.23	1.85
[S II]	4073+	1.	0.05	0.048	0.05	0.014	0.08	0.005
[O III]	4363	0.31	0.01	0.01	0.005	7(-4)	0.067	0.25
He II	4686	0.17	0.17	0.17	1.	0.0026	0.98	0.43
[O III]	5007+	4.6	6.4	6.18	2.5	0.68	8.1	28.8
[N I]	5200+	0.53	1.4(-6)	1.4(6)	0.0	1(-6)	0.0	0.0
He I	5876	0.25	0.13	0.13	0.027	0.17	0.029	0.087
[Fe VII]	6087	0.4	0.008	0.0075	0.005	5(-4)	0.029	1.2
[O I]	6300+	3.5	7(-5)	6.5(-5)	9(-6)	0.074	4(-7)	3.7(-5)
[Fe X]	6374	0.78	2.7(-4)	2.6(-4)	7(-5)	6(-5)	3(-5)	0.003
[N II]	6548+	3.3	0.0039	0.0037	0.001	0.5	7.5(-4)	0.029
[S II]	6716	2.5	0.024	0.023	0.025	0.014	0.03	0.0016
[S II]	6731	4.	0.052	0.05	0.053	0.028	0.068	0.0033
[O II]	7325	0.7	0.00139	0.0011	2(-4)	0.015	4(-4)	0.015
[Fe XI]	7892	0.16	7.5(-5)	7.2(-5)	2(-5)	1.6(-5)	4(-6)	3(-4)
Hβ	$erg\,cm^{-2}s^{-1}$	0.007	11.5	11.8	42.6	46.5	35.	8.19
[S III]	9532+	0.24	0.82	0.81	0.83	0.56	1.	0.99
[C I]	9850	2.77	0.0	0.0	0.0	2.6(-7)	0.0	0.0
[S VIII]	9913	0.13	2(-4)	1.8(-4)	9(-5)	2.4(-5)	5.5(-4)	0.11
[S IX]	1.25	0.11	4(-5)	3.5(-5)	9(-6)	7(-6)	2.2(-5)	0.014
[Si VI]	1.96	0.06	0.016	0.015	0.014	0.0035	0.035	0.65
[Si VII]	2.48	0.19	0.003	0.001	6.7(-4)	1.7(-4)	0.0036	0.13
[Si IX]	2.59	0.65	2.2(-4)	2(-4)	5(-5)	3.3(-5)	7(-5)	0.0135
[Mg VIII]	3.03	0.18	7.7(-5)	7.4(-5)	3(-5)	2.4(-5)	3.6(-4)	0.0054
[Si IX]	3.9	1.2	4(-4)	4(-4)	1(-4)	6.2(-5)	1.8(-4)	0.027
[Mg VII]	5.5	0.14	0.001	9(-4)	5(-4)	1.5(-4)	0.0056	0.049
[Mg V]	5.6	0.025	0.155	0.15	0.14	0.05	0.23	0.44
[Ne VI]	7.6	0.2	0.0016	0.14	1(-4)	4(-5)	0.014	0.76
[Ar III]	8.99	0.011	0.14	0.14	0.15	0.17	0.13	0.08
[S IV]	10.54	0.025	0.89	0.88	0.84	0.5	1.	2.27
[Ne II]	12.8	1.88	0.13	0.13	0.036	0.38	0.015	0.0017
[Ne V]	14.32	0.055	0.0014	0.0012	6(-4)	2.7(-4)	0.12	0.8
[Ne III]	15.55	2.	0.96	0.94	1.17	0.116	1.33	1.06
[S III]	18.7	0.014	0.13	0.13	0.13	0.17	0.12	0.07
[Ne V]	24.3	0.063	5.5(-4)	5(-4)	1.7(-4)	8(-5)	0.036	0.57
[O IV]	25.9	0.135	0.94	0.91	3.14	0.005	3.8	10.
[Fe II]	26.	4.2	3(-4)	3(-4)	3(-4)	0.023	1.3(-4)	3(-6)
[S III]	33.5	0.003	0.019	0.019	0.018	0.028	0.018	0.015
[Si II]	34.86	8.19	0.007	0.007	0.007	0.03	0.005	0.0013
[Ne III]	36.01	0.15	0.056	0.054	0.066	0.0066	0.08	0.065
[O III]	51.81	0.021	0.34	0.34	0.13	0.094	0.15	0.4
[O I]	63.18	8.23	2.3(-6)	2(-6)	4(-7)	0.011	1.6(-8)	1(-6)
[O III]	88.36	0.003	0.04	0.039	0.015	0.011	0.017	0.046
[O I]	145.5	0.41	7(-8)	6(-8)	1(-8)	4(-4)	5(-10)	3.5(-8)
[C II]	157.7	0.3	1.6(-6)	1.6(-6)	7.6(-7)	5.3(-4)	2(-7)	2(-5)

Table 10

The models : V_s=500 $km\,s^{-1}$, n_0=300 cm^{-3}, D= 10^{19}cm

		77	78	79	80	81	82	83
log F_h		SD	8	9	10	11	12	12.7
O VI	1033	131.	0.009	0.01	0.032	0.0013	2(-4)	0.09
Si III	1206	2.4	0.008	0.01	0.002	8(-6)	0.002	0.033
H I	1216	32.6	29.	29.	34.7	29.	29.	29.
N V	1240	6.1	2.7(-4)	3(-4)	9(-4)	3(-5)	6(-4)	0.039
S II	1256	0.22	0.0013	0.002	8(-4)	9(-6)	1.2(-4)	0.0025
Si II	1264	0.055	5(-4)	8(-4)	0.0027	3(-5)	5(-5)	0.001
O I	1302+	0.0033	6(-6)	1.5(-5)	0.003	4(-5)	0.0	2(-5)
Si IV	1397	1.17	0.007	0.007	0.003	2(-5)	0.0015	0.015
O IV	1401+	8.8	0.017	0.015	0.02	4(-6)	0.007	0.049
N IV]	1486	2.5	0.014	0.013	0.017	4.5(-6)	0.006	0.05
C IV	1550	12.6	0.186	0.17	0.23	4(-5)	0.08	0.46
He II	1640	2.1	0.67	0.71	2.8	0.034	5.3	0.95
Si III	1892+	2.05	0.37	0.46	0.084	7(-4)	0.038	0.18
[Ne V]	3426	0.98	3(-4)	2.6(-4)	2.7(-4)	1.4(-5)	0.003	0.06
[O II]	3727	3.2	3.7	4.4	3.2	0.09	0.08	0.33
[Ne III]	3869+	1.04	0.24	0.26	0.58	9(-3)	0.21	0.34
[S II]	4073+	1.0	0.18	0.2	0.14	0.01	0.026	0.045
[O III]	4363	0.31	0.0033	0.0026	0.0023	3.5(-4)	0.005	0.036
He II	4686	0.17	0.1	0.11	0.43	5.4(-3)	0.85	0.15
[O III]	5007+	4.6	0.7	0.51	0.67	0.68	2.1	9.7
[N I]	5200+	0.53	1.3(-4)	2.1(-4)	0.2	3.5(-6)	0.0	0.0
He I	5876	0.22	0.1	0.075	0.09	0.17	0.05	0.13
[Fe VII]	6087	0.41	0.01	0.0094	0.0036	5(-4)	0.0044	0.033
[O I]	6300+	3.54	0.0033	0.007	2.9	0.04	1(-6)	0.014
[Fe X]	6374	0.78	3(-5)	3(-5)	1(-4)	4(-6)	2.4(-6)	2.5(-4)
[N II]	6548+	3.34	4.24	4.7	4.4	0.39	0.13	0.38
[S II]	6716	2.58	0.076	0.09	0.13	0.01	0.016	0.022
[S II]	6731	4.06	0.16	0.18	0.26	0.022	0.034	0.047
[O II]	7325	0.79	0.81	0.99	0.31	0.006	0.012	0.06
[Fe XI]	7892	0.16	8(-6)	1.2(-7)	3(-5)	1.2(-6)	2.3(-7)	4.2(-5)
Hβ	$erg\,cm^{-2}s^{-1}$	0.0067	108.	104.	28.9	640.	613.	474.
[S III]	9532+	0.24	2.56	2.9	5.7	0.44	0.57	0.81
[C I]	9850	2.8	1.4(-5)	1.6(-5)	1.6(-5)	5(-8)	0.0	1.8(-7)
[S VIII]	9913	0.13	8(-5)	6.7(-5)	7.3(-5)	1.25(-5)	1.2(-4)	0.0013
[S IX]	1.25	0.11	4(-6)	4(-6)	1.3(-5)	6(-7)	5(-6)	1.3(-4)
[Si VI]	1.96	0.06	0.007	0.005	0.007	0.004	0.012	0.048
[Si VII]	2.48	0.19	3.7(-4)	3(-4)	4.3(-4)	1.7(-4)	0.001	0.01
[Si IX]	2.59	0.65	2.3(-5)	2.4(-5)	8(-5)	2.4(-6)	1.3(-5)	7.7(-4)
[Mg VIII]	3.03	0.18	8.5(-6)	8.8(-6)	3.6(-5)	4.4(-6)	1(-4)	0.003
[Si IX]	3.9	1.22	4.4(-5)	4.5(-5)	1.5(-4)	4.5(-6)	4(-5)	0.0022
[Mg VII]	5.5	0.144	1.5(-4)	1.4(-4)	3.5(-4)	1.5(-4)	0.0017	0.022
[Mg V]	5.6	0.025	0.026	0.023	0.065	0.06	0.115	0.23
[Ne VI]	7.6	0.21	1.8(-4)	1.6(-4)	1.2(-4)	3.3(-6)	4.3(-4)	0.03
[Ar III]	8.99	0.01	0.22	0.24	0.57	0.15	0.13	0.12
[S IV]	10.54	0.025	0.33	0.27	0.38	0.55	0.67	0.8
[Ne II]	12.8	1.94	0.47	0.47	0.6	0.38	0.07	0.23
[Ne V]	14.32	0.056	1.6(-4)	1.6(-4)	4.1(-4)	1.5(-4)	0.019	0.11
[Ne III]	15.55	2.06	0.25	0.26	0.92	0.1	0.95	0.69
[S III]	18.7	0.014	0.32	0.35	1.23	0.14	0.12	0.12
[Ne V]	24.3	0.063	6(-5)	6(-5)	1.3(-4)	3.5(-5)	0.005	0.033
[O IV]	25.9	0.136	0.48	0.49	1.7	0.0055	1.6	0.26
[Fe II]	26.	3.7	8(-4)	0.0016	0.54	0.0095	4(-4)	0.0055
[S III]	33.5	0.003	0.05	0.056	0.3	0.022	0.017	0.018
[Si II]	34.86	6.44	0.013	0.018	0.36	0.02	0.01	0.01
[Ne III]	36.01	0.158	0.015	0.016	0.06	0.005	0.05	0.04
[O III]	51.81	0.02	0.016	0.011	0.019	0.1	0.17	0.35
[O I]	63.18	7.5	2(-4)	3.7(-4)	0.4	0.0063	1.4(-7)	0.001
[O III]	88.36	0.003	0.002	0.0013	0.0022	0.012	0.019	0.04
[O I]	145.5	0.37	6(-6)	1.1(-5)	0.014	2.2(-4)	4(-9)	3(-5)
[C II]	157.7	0.2	0.002	0.0022	0.009	2.6(-4)	1(-4)	1.6(-4)

Table 11

The models : V_s=1000 $km\,s^{-1}$, n_0=1000 cm^{-3}, F_h=0

		84	85	86	87	88*
D	(10^{17} cm)	3.8719	3.872	3.872	4.133	0.18
T	(10^4 K)	54.5	6.6	2.9	0.029	0.02
O VI	1033	321.	363.	361.	35.2	387.
Si III	1206	0.0	0.06	1.03	0.12	2.00
H I	1215	13.67	14.3	15.3	41.4	19.2
N V	1240	9.76	12.	11.9	1.16	14.22
S II	1256	0.0	0.003	0.056	0.02	0.135
Si II	1264	0.0	3.6(-4)	0.019	0.007	0.04
O I	1302+	0.0	9(-5)	4(-4)	0.004	0.0016
Si IV	1397	3(-5)	0.2	0.5	0.05	1.095
O IV	1401+	6(-5)	4.	4.6	0.46	6.26
N IV]	1486	1.4(-3)	1.	1.1	0.13	1.7
C IV	1550	4.46	8.67	9.88	0.98	3.78
He II	1640	1.0	10.3	10.3	1.34	10.08
Si III	1892+	0.0	0.019	0.7	0.12	1.5
[Ne V]	3426	0.0017	0.48	0.51	0.05	0.54
[O II]	3727	0.0	0.0033	0.015	0.75	0.28
[Ne III]	3869+	0.0	0.045	0.11	0.87	0.18
[S II]	4073+	0.0	1.5(-4)	0.01	2.6	0.06
[O III]	4363	0.0	0.077	0.16	0.021	0.24
He II	4686	0.52	0.53	0.5	0.1	0.53
[O III]	5007+	0.0	0.63	1.5	0.32	3.12
[N I]	5200+	0.0	0.0	0.0	0.13	4.(-5)
He I	5876	0.001	0.0019	0.003	0.11	0.008
[Fe VII]	6087	0.83	0.96	0.95	0.093	0.77
[O I]	6300+	0.0	2.4(-5)	2(-4)	5.72	0.006
[Fe X]	6374	11.75	11.6	11.6	1.13	12.75
[N II]	6548+	0.0	0.0024	0.022	4.0	0.14
[S II]	6716	0.0	4.3(-6)	2.3(-4)	0.7	0.006
[S II]	6731	0.0	1(-5)	5.5(-4)	1.5	0.0136
[O II]	7325	0.0	0.0155	0.1	0.64	0.406
[Fe XI]	7892	2.2	2.16	2.15	0.21	2.66
Hβ	$erg\,cm^{-2}s^{-1}$	0.09	0.093	0.093	0.96	0.02
[S III]	9532+	0.0	0.01	0.07	0.0091	0.18
[C I]	9850	0.0	3(-7)	4.4(-5)	0.16	1.4(-4)
[S VIII]	9913	1.8	1.79	1.78	0.17	1.69
[S IX]	1.25	1.68	1.66	1.65	0.16	1.79
[Si VI]	1.96	0.07	0.094	0.09	0.0091	0.077
[Si VII]	2.48	1.6	1.6	1.6	0.16	1.37
[Si IX]	2.59	10.1	10.	9.93	0.97	10.88
[Mg VIII]	3.03	1.73	1.72	1.7	0.17	1.26
[Si IX]	3.9	18.8	18.6	18.5	1.8	20.3
[Mg VII]	5.5	0.41	0.44	0.44	0.04	0.28
[Mg V]	5.6	2.6(-4)	0.012	0.012	0.0012	0.015
[Ne VI]	7.6	0.0057	0.096	0.096	0.0093	0.077
[Ar III]	8.99	0.0	3(-4)	0.002	3(-4)	0.0067
[S IV]	10.54	0.0	2.6(-3)	0.003	3.3(-4)	0.0149
[Ne II]	12.8	0.0	2.8(-5)	1(-4)	1.35	4.(-4)
[Ne V]	14.32	6(-5)	0.02	0.02	0.0023	0.04
[Ne III]	15.55	0.0	0.0012	0.004	1.28	0.0156
[S III]	18.7	0.0	1.2(-4)	7(-4)	1(-4)	0.005
[Ne V]	24.3	5(-5)	0.01	0.01	9.5(-4)	0.02
[O IV]	25.9	2.5(-7)	0.008	0.01	0.001	0.044
[Fe II]	26.	0.0	7(-9)	1(-6)	0.72	2.(-4)
[S III]	33.5	0.0	1.1(-5)	7(-5)	8.6(-6)	6.4(-4)
[Si II]	34.86	0.0	3.4(-8)	6(-6)	0.34	1.9(-4)
[Ne III]	36.01	0.0	5(-5)	1.5(-4)	0.062	8.2(-4)
[O III]	51.81	0.0	2.8(-4)	7(-4)	4.6(-4)	0.0045
[O I]	63.18	0.0	1.2(-8)	1(-7)	0.64	3.(-5)
[O III]	88.36	0.0	.8(-5)	6.5(-5)	4.7(-5)	4.9(-4)
[O I]	145.5	0.0	0.0	3(-9)	0.019	0.0
[C II]	157.7	0.0	1.9(-8)	8(-7)	0.008	0.0

* Model 72 corresponds to V_s=1500 $km\,s^{-1}$, n_0=300 cm^{-3}, F_h=0

Table 12
The models : V_s=1500 $km\,s^{-1}$, n_0=1000 cm^{-3}, F_h=0

		89	90	91	92	93
D	(10^{17} cm)	7.310	7.311	7.311	7.311	100.
T	(10^4 K)	144.	17.4	2.74	1.3	0.029
O VI	1033	33.5	264.	264.	263.	140.
Si III	1206	0.0	1.4(-5)	0.11	0.125	0.07
H I	1216	11.5	15.4	15.5	15.7	51.3
N V	1240	0.4	7.4	7.5	7.48	4.
S II	1256	0.0	0.0	0.007	0.011	0.024
Si II	1264	0.0	0.0	0.002	0.0028	0.01
O I	1302+	0.0	0.0	2.7(-5)	3.4(-5)	0.009
Si IV	1397	0.0	0.0015	0.05	0.005	0.028
O IV	1401+	0.0	0.11	0.48	0.48	0.25
N IV]	1486	0.0	0.005	0.012	0.11	0.05
C IV	1550	0.05	2.7	3.12	3.14	1.67
He II	1640	10.2	10.3	10.3	10.3	5.87
Si III	1892+	0.0	1.2(-6)	0.08	0.11	0.077
[Ne V]	3426	0.0	0.04	0.05	0.05	0.028
[O II]	3727	0.0	5(-7)	8(-4)	0.002	0.5
[Ne III]	3869+	0.0	1.9(-4)	0.008	0.017	1.1
[S II]	4073+	0.0	0.0	0.0014	0.009	2.6
[O III]	4363	0.0	2(-4)	0.017	0.0021	0.014
He II	4686	0.47	0.53	0.52	0.53	0.34
[O III]	5007+	0.0	0.0015	0.14	0.21	0.27
[N I]	5200+	0.0	0.0	0.0	0.0	0.15
He I	5876	3(-4)	0.001	0.0011	0.0013	0.086
[Fe VII]	6087	0.007	0.65	0.65	0.65	0.34
[O I]	6300+	0.0	0.0	1.2(-5)	2(-4)	6.8
[Fe X]	6374	4.37	11.8	11.8	11.8	6.28
[N II]	6548+	0.0	0.0	0.0013	0.0035	5.23
[S II]	6716	0.0	0.0	2(-5)	1.5(-4)	0.89
[S II]	6731	0.0	0.0	5(-5)	3.6(-4)	1.88
[O II]	7325	0.0	3(-6)	0.006	0.012	0.5
[Fe XI]	7892	2.53	2.6	2.59	2.58	1.37
Hβ	$erg\,cm^{-2}s^{-1}$	0.3	1.38	1.38	1.39	2.6
[S III]	9532+	0.0	5.6(-7)	0.007	0.009	0.005
[C I]	9850	0.0	0.0	2.7(-6)	7(-6)	0.03
[S VIII]	9913	0.045	1.59	1.59	1.59	0.84
[S IX]	1.25	0.22	1.6	1.61	1.61	0.86
[Si VI]	1.96	1.9(-5)	0.053	0.05	0.05	0.028
[Si VII]	2.48	0.0022	1.32	1.33	1.32	0.7
[Si IX]	2.59	0.3	9.6	9.6	9.58	5.1
[Mg VIII]	3.03	0.005	1.32	1.32	1.32	0.7
[Si IX]	3.9	0.56	17.8	17.8	17.8	9.45
[Mg VII]	5.5	1.7(-4)	0.28	0.28	0.28	0.15
[Mg V]	5.6	0.0	0.0012	0.0012	0.0012	6(-4)
[Ne VI]	7.6	1.4(-5)	0.01	0.01	0.011	0.006
[Ar III]	8.99	0.0	3(-7)	2(-4)	2.6(-4)	1.9(-4)
[S IV]	10.54	0.0	1.3(-6)	2.4(-4)	2.4(-4)	1.3(-4)
[Ne II]	12.8	0.0	1.2(-8)	5(-6)	3(-5)	1.5
[Ne V]	14.32	0.0	0.0015	0.0019	0.0019	0.001
[Ne III]	15.55	0.0	4(-6)	2(-4)	0.001	1.78
[S III]	18.7	0.0	6(-9)	5.6(-5)	6.7(-5)	4(-5)
[Ne V]	24.3	0.0	5(-4)	5.7(-4)	5.7(-4)	3(-4)
[O IV]	25.9	0.0	1.4(-4)	7(-4)	7.6(-4)	4(-4)
[Fe II]	26.	0.0	0.0	1(-7)	1(-5)	1.62
[S III]	33.5	0.0	0.0	5(-6)	6(-6)	3(-6)
[Si II]	34.86	0.0	0.0	5.2(-7)	7(-6)	1.04
[Ne III]	36.01	0.0	1.9(-7)	8(-6)	3(-5)	0.10
[O III]	51.81	0.0	6(-7)	4.2(-5)	1(-4)	4(-4)
[O I]	63.18	0.0	0.0	0.0	3.5(-7)	2.18
[O III]	88.36	0.0	6(-8)	4(-6)	9(-6)	4(-5)
[O I]	145.5	0.0	0.0	0.0	1(-8)	0.064
[C II]	157.7	0.0	0.0	0.0	1.4(-7)	0.027

Table 13

Maximum densities and temperatures downstream

V_s ($km\,s^{-1}$)	n_0 (cm^{-3})	n(max) (cm^{-3})	T(max) (K)
100	100	618.	1.5(5)
100	300	3176.	1.5(5)
200	200	3723.	6.0(5)
300	300	1.04(4)	1.35(6)
500	300	1.75(4)	3.75(6)
1000	1000	2.1(5)	1.5(7)
1500	1000	3.2(5)	3.4(7)

Table 14

Line ratios for SD models

Vs	n_0	[OIII]5007+/[OII]3727	[OIII]5007+/4363	[SII]6717/6730	[SiIX]3.9/[SiVII]2.48	[NeIII]15.5/[NeII]12.8
100	100	0.38	12.45 - 12.9	1.04	-	0.45 - 0.16
100	300	0.46	12.5	0.68	-	0.64
200	200	0.59	12.35	0.64	-	0.86
300	300	1.04	12.7	0.66	1.5	1.16 - 1.04
500	300	1.43	14.8	0.63	6.3	6.3
1000	1000	0.43	15.2	0.47	11.2	0.95
1500	1500	0.54	19.3	0.47	13.5	1.18